

FSU-HEP-000216
 UCCHEP/12-00
 IFIC/00-18
 FTUV/000504
 UH-511-963-00

YUKAWA UNIFIED SUPERSYMMETRIC $SO(10)$ MODEL: COSMOLOGY, RARE DECAYS AND COLLIDER SEARCHES

Howard Baer¹, Michal Brhlik², Marco A. Díaz³, Javier Ferrandis⁴,
 Pedro Mercadante¹, Pamela Quintana¹ and Xerxes Tata⁵

¹*Department of Physics, Florida State University, Tallahassee, FL 32306 USA*

²*Randall Physics Laboratory University of Michigan, Ann Arbor, MI 48109-1120 USA*

³*Facultad de Física, Universidad Católica de Chile, Av. Vicuña Mackenna 4860, Santiago, Chile*

⁴*Departament de Física Teòrica, Universitat de València, Spain*

⁵*Department of Physics and Astronomy, University of Hawaii, Honolulu, HI 96822, USA*

(April 26, 2024)

Abstract

It has recently been pointed out that viable sparticle mass spectra can be generated in Yukawa unified $SO(10)$ supersymmetric grand unified models consistent with radiative breaking of electroweak symmetry. Model solutions are obtained only if $\tan\beta \sim 50$, $\mu < 0$ and positive D -term contributions to scalar masses from $SO(10)$ gauge symmetry breaking are used. In this paper, we attempt to systematize the parameter space regions where solutions are obtained. We go on to calculate the relic density of neutralinos as a function of parameter space. No regions of the parameter space explored were actually cosmologically excluded, and very reasonable relic densities were found in much of parameter space. Direct neutralino detection rates could exceed 1 event/kg/day for a ^{73}Ge detector, for low values of GUT scale gaugino mass $m_{1/2}$. We also calculate the branching fraction for $b \rightarrow s\gamma$ decays, and find that it is beyond the 95% CL experimental limits in much, but not all, of the parameter space regions explored. However, recent claims have been made that NLO effects can reverse the signs of certain amplitudes in the $b \rightarrow s\gamma$ calculation, leading to agreement between theory and experiment in Yukawa unified SUSY models. For the Fermilab Tevatron collider, significant regions of parameter space can be explored via $b\bar{b}A$ and $b\bar{b}H$ searches. There also exist some limited regions of parameter space where a trilepton signal can be seen at TeV33. Finally, there exist significant regions of parameter space where direct detection of bottom squark pair production can be made, especially for large negative values of the GUT parameter A_0 .

PACS numbers: 14.80.Ly, 13.85.Qk, 11.30.Pb

Typeset using REVTeX

I. INTRODUCTION

Supersymmetric $SO(10)$ grand unified theories [1] (GUTS) are highly motivated choices for particle physics models which encompass and go beyond the Standard Model (SM). In particular:

- All three forces in the SM are unified by a simple Lie group. Since the model is supersymmetric, the hierarchy between weak and GUT scales is naturally stabilized.
- The fifteen distinct fermions of each SM generation plus a SM gauge singlet right-handed neutrino state are economically included in the sixteen dimensional spinorial representation of $SO(10)$.
- The group $SO(10)$ is anomaly-free, and provides an explanation for cancellation of triangle anomalies that are otherwise rather ad-hoc in both the MSSM and $SU(5)$ SUSY-GUT models.
- The SM weak hypercharge assignments can be derived from broken $SO(10)$ using only the lowest dimensional $SO(10)$ Higgs multiplets. This has been interpreted as group theoretic evidence of $SO(10)$ grand unification [2].
- The singlet neutrino superfield(s) \hat{N}^c may develop a Majorana mass at very high energy scales $\sim 10^{11} - 10^{16}$ GeV. Combining these with the usual Dirac neutrino masses that can now develop, one is lead to (dominantly) left-handed neutrino masses at the eV scale (or below), while right handed neutrinos are pushed beyond observability, via the see-saw mechanism [3]. The resulting neutrino masses can easily be in accord with recent data from solar and atmospheric neutrino detection experiments, though a detailed model is necessary for an explanation of the observed mixing pattern.
- In minimal $SO(10)$, there exists only a single Yukawa coupling per generation, so that Yukawa couplings also unify at the GUT scale. This is especially constraining for the third generation. In addition, predictive $SO(10)$ models can be created which encompass the fermion masses of the lighter generations as well [4].
- In $SO(10)$ models, R -parity conservation is a natural consequence of the gauge symmetry of the model [5]. When $SO(10)$ is broken, if the breaking occurs via certain “safe” representations of the Higgs fields, R -parity is still conserved even in the weak scale theory [6]. Along the same lines, it has been shown that in SUSY models with gauged $B - L$ (this includes $SO(10)$ models) symmetry and a renormalizable see-saw mechanism, R -parity must be conserved exactly, even in the weak scale Lagrangian [7].
- In $SO(10)$ models, baryogenesis in the early universe can be explained as a consequence of decays of (out of thermal equilibrium) intermediate scale right-handed neutrino states [8].

Motivated by these considerations, in this paper we investigate a variety of phenomenological implications of Yukawa-unified $SO(10)$ SUSY-GUT models. Throughout our study, we assume the following:

1. A minimal $SO(10)$ SUSY GUT model with a single Yukawa coupling per generation, valid at energy scales $Q > M_{GUT} \simeq 2 \times 10^{16}$ GeV.
2. The gauge symmetry $SO(10)$ breaks via some (to be specified) mechanism directly to the MSSM gauge group at $Q = M_{GUT}$. We assume universality of soft SUSY breaking mass parameters at $Q = M_{GUT}$. However, as a consequence of the reduction in rank of the gauge symmetry breaking, additional D -term mass contributions are generated for scalar masses.
3. Electroweak symmetry is broken radiatively (REWSB).

With these assumptions, the spectrum of supersymmetric particles and Higgs bosons can be calculated. We examine various phenomenological consequences of the sparticle mass spectrum generated. We do not address the related question of mass generation of first and second generation SM fermions; this issue has been investigated in a number of other papers [4]. We also do not explore the specific mechanisms involved in gauge symmetry breaking; several studies along these lines are contained in Ref. [9].

A crucial issue is to find models with Yukawa coupling unification which reproduce the observed masses for the third generation fermions. One may assume Yukawa unification at $Q = M_{GUT}$, and evolve gauge and Yukawa couplings and soft SUSY breaking (SSB) masses to the weak scale, and only accept solutions which generate third generation fermion masses in agreement with measurements within tolerances. Alternatively, one may begin with the central values of measured fermion masses at low energies, and accept only solutions which give Yukawa unification to within set tolerances at the GUT scale. In this paper, we adopt the latter bottom-up approach. A crucial aspect for this approach is to correctly calculate the weak scale third generation Yukawa couplings. Throughout our work, we fix pole masses $m_b = 4.9$ GeV, $m_t = 175$ GeV and $m_\tau = 1.78$ GeV.

The mass spectrum of SUSY particles in minimal supersymmetric $SO(10)$ constrained by radiative electroweak symmetry breaking has been studied previously in a number of papers [10–20]. Unification of bottom, tau and top Yukawa couplings was found to occur at very large values of the parameter $\tan \beta \sim 50 - 60$, and specific spectra were generated for values of $m_t \sim 190$ GeV [11]. Assuming universality of soft SUSY breaking masses at M_{GUT} , it was found [12,14] that Yukawa unification consistent with radiative electroweak symmetry breaking could also occur for $m_t < 170$ GeV as long as $m_{1/2} \gtrsim 300$ GeV. This generally leads to sparticle masses far beyond the reach of the CERN LEP2 or Fermilab Tevatron $p\bar{p}$ colliders. For values of $m_t \simeq 175$ GeV, solutions including radiative electroweak breaking were very difficult to achieve. In Ref. [19], the SUSY particle mass spectrum was investigated with *non-universal* SSB masses. Various solutions were found, but ad hoc non-universality conflicts with the $SO(10)$ symmetry. In Ref. [20], it was suggested that $SO(10)$ D -term contributions to scalar masses had the correct form to allow for successful radiative electroweak symmetry breaking and the computation of weak scale SUSY particle masses, but explicit solutions were not presented.

In a previous paper [21], we have shown that Yukawa unified solutions to the superparticle mass spectrum could be generated (even for $m_t = 175$ GeV) assuming universality within $SO(10)$, but only if additional D -term contributions to scalar masses were included. Solutions with Yukawa unification good to 5% and REWSB were found only for values of

$\mu < 0$ and positive values of the D -term contributions. A crucial ingredient in the calculation is the inclusion of SUSY loop corrections to fermion masses [15,12,22], from which the third generation weak scale Yukawa couplings are calculated. For $\mu > 0$, the diminution in the b -quark Yukawa coupling is so severe that not even $b - \tau$ unification can be achieved for any values of $\tan\beta : 2 - 60$. For values of $\tan\beta \gtrsim 60$, the Yukawa couplings diverge during renormalization group running from the weak scale to the GUT scale, so that these values of $\tan\beta$ form an upper limit to the allowed parameter space. For $\mu < 0$, assuming universality of SSB scalar masses, a much lower parameter space limit of $\tan\beta \lesssim 45$ is found. For higher values of $\tan\beta$ we find $\mu^2 < 0$, and REWSB falters essentially because the Higgs mass squared $m_{H_d}^2$ is driven to smaller weak scale values than $m_{H_u}^2$. However, if one allows positive D -term contributions to scalar masses, then $m_{H_u}^2 < m_{H_d}^2$ already at M_{GUT} , and the region of allowed $\tan\beta$ expands to $\tan\beta \sim 50 - 55$. This is sufficient to allow for $t - b - \tau$ Yukawa unification for many models with $\mu < 0$. Of course, the D -term contributions must be added to the various squark and slepton soft masses as well, so that the D -terms leave a distinctive imprint on the superparticle mass spectrum [23]. The most striking possibility is that the light bottom squark could be by far the lightest of all the squarks, and furthermore, even within range of Fermilab Tevatron searches. In addition, left- slepton masses could be lighter than right slepton masses, in contrast to expectations from the SUSY models with universality at $Q = M_{GUT}$. This latter effect could certainly be extracted from precision measurements at linear e^+e^- colliders operating at $\sqrt{s} \gtrsim 1$ TeV, and would be evidence in favor of a Yukawa unified $SO(10)$ SUSY GUT model.

In this paper, we address many of the observable aspects of Yukawa-unified $SO(10)$ models in some detail. In Sec. II, we summarize the results from Ref. [21], and try to systematize the parameter space expected in Yukawa unified $SO(10)$ model framework. In Sec. III, we present calculations of the cosmological relic density of neutralinos in this class of models. Over much of the parameter space, we find very reasonable relic densities, unless $m_{\tilde{Z}_1} \simeq \frac{m_A}{2}$, where s -channel annihilation through a Higgs resonance can lower Ωh^2 to very tiny values. Given a reasonable relic density, it is well-known that rates for direct neutralino detection experiments are highest at large $\tan\beta$. We show direct detection rates in $SO(10)$ parameter space, and show that much of the space should be explorable by neutralino-nucleon scattering experiments. In Sec. IV, we evaluate the rate for $b \rightarrow s\gamma$ decays. Much of the parameter space is excluded by the measured value of the branching fraction for the decay $b \rightarrow s\gamma$, but some distinctive regions remain viable. These results may be subject to modification if there is additional non-universality or inter-generational squark mixing at $Q = M_{GUT}$, or if CP violating phases are significant. In addition, recent claims have been made that NLO QCD corrections to $b \rightarrow s\gamma$ loop diagrams can reverse the signs of certain amplitudes, leading to *agreement* between experimental measurements and theory predictions from Yukawa unified SUSY models. In Sec. V, we examine regions of parameter space accessible to searches for supersymmetry at the Fermilab Tevatron collider. We find three possibilities: *i*) signals from $A\tilde{b}\tilde{b}$ or $H\tilde{b}\tilde{b}$ associated production, *ii*) $\tilde{W}_1\tilde{Z}_2 \rightarrow 3\ell$ signals if $\tan\beta$ is not too big, and *iii*) signals from direct production of $\tilde{b}_1\tilde{\bar{b}}_1$ pairs, where observable rates occur for large negative values of A_0 . Experiments at the Large Hadron Collider (LHC) would, of course, decisively probe the model. We end in Sec. VI with a summary of our results, and some concluding remarks.

II. MINIMAL $SO(10)$ MODEL PARAMETER SPACE

In the minimal supersymmetric $SO(10)$ GUT model, the fifteen matter superfields of each generation of the MSSM plus a gauge singlet neutrino superfield \hat{N}^c are included in the 16-dimensional spinorial representation $\hat{\psi}$ of $SO(10)$. In addition, the two Higgs doublet superfields \hat{H}_u and \hat{H}_d are embedded in a single 10-dimensional Higgs superfield $\hat{\phi}$. The superpotential includes the term

$$\hat{f} \ni f \hat{\psi} \hat{\psi} \hat{\phi} + \dots$$

responsible for quark and lepton masses, with f the single Yukawa coupling per generation in the GUT scale theory. The dots represent terms including for instance higher dimensional Higgs representations and interactions responsible for the breaking of $SO(10)$. We neglect Yukawa couplings and fermion masses for the first two generations. As usual, SUSY breaking, is parametrized by associated soft SUSY breaking mass terms. We assume a common mass m_{16} for all matter scalars and a mass m_{10} for the Higgs scalars, along with a universal gaugino mass $m_{1/2}$, and common trilinear and bilinear SSB masses A_0 and B . Motivated by apparent gauge coupling unification in the MSSM, $SO(10)$ is assumed to break directly to the gauge group $SU(3)_C \times SU(2)_L \times U(1)_Y$ at $Q = M_{GUT}$, where the reduction in rank of the gauge symmetry leads to distinct D -term contributions to scalar field mass terms. The scalar field squared masses at $Q = M_{GUT}$ are then given by

$$\begin{aligned} m_Q^2 &= m_E^2 = m_U^2 = m_{16}^2 + M_D^2 \\ m_D^2 &= m_L^2 = m_{16}^2 - 3M_D^2 \\ m_{H_{u,d}}^2 &= m_{10}^2 \mp 2M_D^2, \end{aligned}$$

where M_D^2 parametrizes the magnitude of the D -terms, and can, owing to our ignorance of the gauge symmetry breaking mechanism, be taken as a free parameter, with either positive or negative values. $|M_D|$ is expected to be of order the weak scale. Thus, the model is characterized by the following free parameters¹:

$$m_{16}, m_{10}, M_D^2, m_{1/2}, A_0, \text{sign}(\mu).$$

The value of $\tan \beta$ will be restricted by the requirement of Yukawa coupling unification, and so is tightly constrained to a narrow range around $\tan \beta \sim 50$.

In our previous paper [21], our procedure was as follows. We generated random samples of model parameter sets within the ranges,

$$\begin{aligned} 0 < m_{16} < 1500 \text{ GeV}, \\ 0 < m_{10} < 1500 \text{ GeV}, \end{aligned}$$

¹If the effective theory below the GUT scale is the MSSM plus a right-handed neutrino, then several other parameters enter the discussion. Typically, these have only a small effect on the SUSY particle mass spectrum: see Ref. [24]

$$\begin{aligned}
0 < m_{1/2} < 500 \text{ GeV}, \\
-500^2 \text{ GeV}^2 < M_D^2 < +500^2 \text{ GeV}^2, \\
45 < \tan \beta < 55, \\
-3000 \text{ GeV} < A_0 < 3000 \text{ GeV} \text{ and} \\
\mu > 0 \text{ or } \mu < 0.
\end{aligned} \tag{2.1}$$

For each parameter set, we then calculated the non-universal scalar masses according to formulae given above, and enter the parameters into the computer program ISASUGRA. ISASUGRA is a part of the ISAJET package [25] which calculates an iterative solution to the 26 coupled RGEs of the MSSM.

To calculate the values of the Yukawa couplings at scale $Q = M_Z$, we began with the pole masses $m_b = 4.9 \text{ GeV}$ and $m_\tau = 1.78 \text{ GeV}$. We calculated the corresponding running masses in the \overline{MS} scheme, and evolve m_b and m_τ up to M_Z using 1-loop SM RGEs. At $Q = M_Z$, we included the SUSY loop corrections to m_b and m_τ using the approximate formulae of Pierce *et al.* [22], and then obtained the corresponding Yukawa couplings. A similar procedure is used to calculate the top quark Yukawa coupling at scale $Q = m_t$. We assume a pole mass $m_t = 175 \text{ GeV}$.

Starting with the three gauge couplings and t , b and τ Yukawa couplings of the MSSM at scale $Q = M_Z$ (or m_t), ISASUGRA evolves the various couplings up in energy until the scale where $g_1 = g_2$, which is identified as M_{GUT} , is reached. The GUT scale boundary conditions are imposed, and the full set of 26 RGE's for gauge couplings, Yukawa couplings and relevant SSB masses are evolved down to $Q \sim M_{weak}$, where the renormalization group improved one-loop effective potential is minimized at an optimized scale choice $Q = \sqrt{m_{\tilde{t}_L} m_{\tilde{t}_R}}$ and radiative electroweak symmetry breaking is imposed. Using the new spectrum, the full set of SSB masses and couplings are evolved back up to M_{GUT} including weak scale sparticle threshold corrections to gauge couplings. The process is repeated iteratively until a stable solution within tolerances is achieved. We accepted only solutions for which the Yukawa couplings f_t , f_b and f_τ unify to within 5%. This constraint effectively fixes the value of $\tan \beta$ to a narrow range of 49 ± 3 . Yukawa unified solutions are found only for values of $\mu < 0$. This latter result is in accord with findings of Pierce *et al.* [22] where solutions for $b - \tau$ unification in models with universality were found only for one sign of μ when $\tan \beta$ was large. We also require the lightest SUSY particle to be the lightest neutralino, and that electroweak symmetry is successfully broken radiatively.

In this paper, we have used upgraded ISAJET 7.47 including 2-loop Yukawa coupling RGEs [26] with weak scale threshold corrections [27] to check our previous solutions. The updated solutions as a function of model parameter space are presented in Fig. 1; no apparent differences can be seen compared with our earlier results which used just 1-loop RGEs for Yukawa coupling evolution. The Yukawa unified solutions to the SUSY particle mass spectra are found to occur typically with $m_{16} \lesssim m_{10} \lesssim 1.5 m_{16}$ and for $0.1 m_{16} \lesssim M_D \lesssim .35 m_{16}$. Too small of a D -term will not yield enough splitting in the Higgs boson soft masses to yield REWSB, while too large a D -term will lead to third generation scalar field masses below experimental limits, or to charge and/or color breaking minima in the scalar potential. Our requirement of 5% unification is determined by defining the variables $r_{b\tau}$, r_{tb} and $r_{t\tau}$, where for instance $r_{b\tau} = \max(f_b/f_\tau, f_\tau/f_b)$. We then require $R = \max(r_{b\tau}, r_{tb}, r_{t\tau}) < 1.05$.

The methodology employed in Ref. [21] is useful for determining the general regions of

model parameter space where Yukawa-unified solutions with REWSB can be found. However, in order to survey the predictions of model parameter space for observable quantities of experimental interest, it is useful to develop a more systematic approach to the model parameter space. For most of the results in this paper, we will take $\tan \beta = 50$ as an indicative central value. We are also restricted to $\mu < 0$. Guided by the results of Fig. 1a, we can also adopt a central value $m_{10} = 1.25m_{16}$, and from Fig. 1b, $M_D = \frac{1}{5}m_{16}$ or $M_D = \frac{1}{3}m_{16}$. Then, most of the variation in parameter space comes from the values of m_{16} and $m_{1/2}$, for which, from Fig. 1c, there is no obvious correlation.

We show in Fig. 2 the resulting m_{16} vs. $m_{1/2}$ plane, taking as well $A_0 = 0$, for a) the smaller and b) the larger value of M_D . The region shaded by solid dots is excluded on the left by negative values of m_A^2 , and on the right by negative values of μ^2 : in either case, the REWSB constraint is violated. The unshaded region gives viable solutions to the superparticle mass spectra, although Yukawa unification can vary throughout the plot from regions with $R < 1.05$ to $R \simeq 1.25$. The value of R can be fine-tuned to less than 1.05 throughout much of the parameter space plane by adjusting the value of $\tan \beta$ within the band in Fig. 1d. To gain an idea of the superparticle and Higgs boson mass spectrum throughout the parameter space plane, we show dashed contours of squark mass $m_{\tilde{u}_L} = 1000$ (lower) and 2000 GeV (upper contour). As noted in Ref. [21], the first and second generation squark masses are bounded below by about 700 GeV, and are usually much heavier in the Yukawa-unified $SO(10)$ model. The chargino mass contours of $m_{\tilde{W}_1} = 150, 250$ and 350 GeV are shown as solid contours, increasing with $m_{1/2}$. They asymptote towards the right-hand parameter space boundary, which is given by solutions where $\mu^2 = 0$. For large values of the weak scale gaugino mass M_2 , $|\mu| \lesssim M_2$, so that the lightest chargino and neutralinos contain significant higgsino components. Although first and second generation squarks and sleptons are quite heavy and beyond the reach of LEP2 and Tevatron experiments, the charginos can be light, and within the reach of these collider facilities. Finally, the dotted contours show values of the pseudoscalar Higgs mass $m_A = 150, 250$ and 350 GeV, from left to right. Regions of parameter space with $m_A \simeq 100 - 200$ GeV and large $\tan \beta$, as in this model, may have Higgs bosons accessible to Fermilab Tevatron collider searches via the $b\bar{b}A$ and $b\bar{b}H$ production mechanisms [28].

In Fig. 3, we show similar plots of model parameter space, this time taking $M_D = \frac{1}{3}m_{16}$, but a) $A_0 = -m_{16}$ and b) $A_0 = +m_{16}$. The mass contours are the same as in Fig. 2. In Ref. [21], it was shown that the light bottom squark \tilde{b}_1 could well be by far the lightest of all the squarks in Yukawa-unified $SO(10)$. For negative A_0 parameters, mixing effects in the bottom squark mass matrix can give rise to even smaller values of $m_{\tilde{b}_1} \sim 100 - 300$ GeV, which may be accessible to direct searches at the Fermilab Tevatron [29]. In addition, as can be seen, the range of parameter space is increased beyond the corresponding result for $A_0 = 0$. Alternatively, taking $A_0 = +m_{16}$ yields typically heavier bottom squark masses, and a smaller range of accessible parameter space.

In Fig. 4, we show again the parameter space plane for $M_D = \frac{1}{3}m_{16}$ but with a) $A_0 = -m_{16}$ and b) $A_0 = 0$. The planes of Fig. 4 shall form the template for most of the results to come in the following sections. We show in Fig. 4 contours of the degree of Yukawa unification R in per cent. The Yukawa unification varied from less than 5% to over 20% throughout the plane. We note that Fig. 1d, makes it evident that for lower values of $m_{1/2}$ we will have better Yukawa coupling unification occurring at slightly lower values of $\tan \beta$

than $\tan\beta = 50$ in this figure.

It was pointed out in [21] that the lightest slepton in this model is the stau, and that solutions with $m_{\tilde{\tau}_1} < 200$ GeV are hard to obtain. This is confirmed in Fig. 5 where we plot the stau mass as a function of the left-right mixing angle in the stau sector. Four different regions are indicated according to the value of the D-term mass parameter M_D (there is some overlap between them in the boundaries). As opposed to models with universality, where the light stau has mainly a right stau component, in SO(10) it can have any value for the mixing angle. In ISAJET, we take $\tilde{\tau}_1 = \cos\theta_\tau\tilde{\tau}_L - \sin\theta_\tau\tilde{\tau}_R$, so that small values of M_D prefer $\cos\theta_\tau \approx 0$ and a dominantly right $\tilde{\tau}_1$, while large values of M_D prefer $\cos\theta_\tau \approx 1$ and a dominantly left $\tilde{\tau}_1$. Any intermediate value of $\cot\theta_\tau$ is also allowed, so that the light stau could be a very mixed state of $\tilde{\tau}_L$ and $\tilde{\tau}_R$.

III. EVALUATION OF NEUTRALINO RELIC DENSITY

Recent precision measurements of cosmological parameters present new and interesting constraints on the possibility of particle cold dark matter [30]. Analyses of the cosmic microwave background radiation suggest a matter/energy density of the universe $\Omega = \frac{\rho}{\rho_c} = 1.0 \pm 0.2$, *i.e.* consistent with a flat universe. In addition, the Hubble constant itself is now estimated as $H_0 = (65 \pm 5)$ km/sec/Mpc, yielding a value $\Omega h^2 \sim 0.42$, where $H_0 = 100h$ km/sec/Mpc with h the scaled Hubble constant. The baryonic contribution to Ωh^2 is estimated to be $\Omega_B h^2 \sim 0.02$ from Big Bang nucleosynthesis (BBN) arguments, while the contribution from neutrinos ought to be $\Omega_\nu h^2 \lesssim 0.06$, mainly from models of structure formation in the universe. Information on the total matter density of the universe can be found by combining constraints from BBN with measurements of intracluster gas and gravitational binding in rich galactic clusters: the results indicate $\Omega_M h^2 \sim 0.17$. The remaining matter density may come from cold dark matter (CDM) particles, while the remaining energy density may come from a non-zero cosmological constant, as is suggested by recent measurements of type Ia supernovae. The lightest neutralino of supersymmetry is an excellent candidate for CDM in the universe. In a universe with 5% each of baryonic matter and massive neutrinos, and a cosmological constant with $\Omega_\Lambda h^2 \sim 0.25$, we would expect $\Omega_{\tilde{Z}_1} h^2 \sim 0.13$. As an extreme, assuming no contribution from the cosmological constant, we would obtain $\Omega_{\tilde{Z}_1} h^2 \sim 0.38$. In order to account only for the dark matter needed to explain galactic rotation curves, we would expect $\Omega_{\tilde{Z}_1} h^2 \gtrsim 0.02$.

To estimate the relic density [31] of neutralinos in Yukawa-unified SO(10), we follow the calculational procedure outlined in Ref. [32]. Briefly, we evaluate all tree level neutralino annihilation diagrams exactly as helicity amplitudes. We then calculate the neutralino annihilation cross section, and compute the thermally averaged cross section times velocity using the fully relativistic formulae of Gondolo and Gelmini [33]. Once the freeze-out temperature is obtained via an iterative solution, we can straightforwardly obtain the neutralino relic density $\Omega_{\tilde{Z}_1} h^2$. Our program takes special care to integrate properly over any Breit-Wigner poles in s -channel annihilation diagrams [32]. We do not include $\tilde{Z}_1 - \tilde{\tau}_1$ co-annihilation diagrams; these can be important in mSUGRA models [34], but are unimportant in the

$SO(10)$ model since the slepton masses are always far heavier than the lightest neutralino.² Our calculations of the relic density also do not include effects that might be significant [36] if the b -squark is sufficiently degenerate with \tilde{Z}_1 .

Our results for the neutralino relic density are shown in Fig. 6 for the same parameters as in Fig. 4. We show contours of $\Omega h^2 = 0.02, 0.1, 0.15, 0.2, 0.25, 0.3$ and 0.35 . In frame a), we see that there exists wide ranges of parameter space for which the relic density $0.02 \lesssim \Omega_{\tilde{Z}_1} h^2 \lesssim 0.35$, *i.e.* in the cosmologically interesting region. In no part of the plane shown does the relic density exceed $\Omega_{\tilde{Z}_1} h^2 = 0.81$. Much of the interesting region of parameter space occurs for large values of scalar masses, which is contrary to the situation at low $\tan \beta$, where large scalar masses suppress the annihilation cross section, and typically yield $\Omega_{\tilde{Z}_1} h^2 > 1$. At large $\tan \beta$, the decay widths of the Higgs bosons H and A become very large, typically $50 - 100$ GeV. Then annihilation can proceed through the very broad s -channel H and A resonances, even if $2m_{\tilde{Z}_1} \neq m_A$ or m_H . In a diagonal swath that splits the allowed parameter space, the relic density drop to $\Omega_{\tilde{Z}_1} h^2 < 0.02$. This trough is due to regions where $m_A \simeq 2m_{\tilde{Z}_1}$, and where annihilation can occur very efficiently through the s -channel diagrams. In frame b), we show similar results except for $A_0 = 0$. Again, we see a region between the $\Omega_{\tilde{Z}_1} h^2 = 0.02$ with very low relic densities. Throughout the remaining parameter space region, the relic density is of cosmologically interesting values, and in fact never exceeds $\Omega_{\tilde{Z}_1} h^2 \sim 0.6$.

IV. DIRECT DETECTION RATES FOR RELIC NEUTRALINOS

A consequence of the SUSY dark matter hypothesis is that a non-relativistic gas of neutralinos fills all space. To test this hypothesis, a number of direct neutralino detection experiments have been built or are under construction [37]. The general idea behind these experiments is that neutralinos (or some other CDM candidate) could elastically scatter off nuclei in some material, transferring typically tens of keV of energy to the recoiling nucleus. Current generation detectors are aiming at a sensitivity of 0.1-0.01 events/kg/day

The first step involved in a neutralino-nucleus scattering calculation is to calculate the effective neutralino-quark and neutralino-gluon interactions. The neutralino-quark axial vector interaction leads in the non-relativistic limit to a neutralino-nucleon spin-spin interaction, which involves the measured quark spin content of the nucleon. To obtain the neutralino-nucleus scattering cross section, a convolution with nuclear spin form factors must be made. The neutralino-quark and neutralino-gluon interactions (via loop diagrams) can also resolve into scalar and tensor components. These interactions can be converted into an effective scalar neutralino-nucleon interaction involving quark and gluon parton distribution functions. A neutralino-nucleus scattering cross section can be obtained by convoluting with suitable scalar nuclear form factors. The final neutralino detection rate is obtained by

²Recently, two papers have appeared on calculating the relic density in Yukawa unified $SO(10)$ [35]. Since these authors do not insist on correct third generation fermion masses, they are able to obtain sparticle mass spectra without invoking D -terms. Thus, their results differ significantly from ours.

multiplying by the *local* neutralino density (for which estimates are obtained from galaxy formation modeling), and appropriate functions involving the velocity distribution of relic neutralinos and the earth's velocity around the galactic center.

In this section, we present event rates for direct detection of relic neutralinos left over from the Big Bang. For illustration, we present detailed calculations for a ^{73}Ge detector, which has a sizable nuclear spin content $J = \frac{9}{2}$. We follow the procedures outlined in Ref. [38], and assume a local neutralino density $\rho_{\tilde{Z}_1} = 5 \times 10^{-25} \text{ g cm}^{-3}$ [39].

Our results are shown in Fig. 7 for the same parameter plane as in Fig. 4. We show direct detection rate contours of 1, 0.1, 0.01 and 0.001 events/kg/day. In the low $m_{1/2}$ regions of parameter space, the direct detection rate exceeds 1 event/kg/day, which is a very large rate for neutralino dark matter. The large rate occurs generically at large $\tan\beta$ [40,38]. Neutralinos can scatter off quarks via squark or Higgs boson exchange graphs, and off gluons via loop graphs containing quarks, squarks and gluons. Neutralino-gluon scattering via Higgs exchange into a b -quark loop for instance is enhanced at large $\tan\beta$, and helps lead to the large scattering rate. Unfortunately, the largest direct detection rates occur mainly in those regions of parameter space where the relic density is tiny. However, there do exist significant regions of parameter space where the direct neutralino detection rate exceeds 0.01 events/kg/day where the relic density is comfortably within the cosmologically interesting range.

V. CONSTRAINT FROM RADIATIVE B DECAY

A. Results for $BR(b \rightarrow s\gamma)$

The radiative flavor-changing decay $b \rightarrow s\gamma$ can occur in the SM via Wt loop diagrams; in SUSY theories, additional diagrams including tH^+ , $\tilde{W}_i\tilde{t}_j$, $\tilde{g}\tilde{q}$ and $\tilde{Z}_i\tilde{q}$ loops will occur [41,42]. The ALEPH collaboration [43] has measured

$$BR(b \rightarrow s\gamma) = (3.11 \pm 0.80 \pm 0.72) \times 10^{-4} \quad (5.1)$$

while the CLEO collaboration [44] has recently reported

$$BR(b \rightarrow s\gamma) = (3.15 \pm 0.35 \pm 0.32 \pm 0.26) \times 10^{-4} \quad (5.2)$$

and restricts the branching ratio at 95% CL to be

$$2 \times 10^{-4} < BR(b \rightarrow s\gamma) < 4.5 \times 10^{-4}. \quad (5.3)$$

The SM prediction at NLL accuracy [45] is

$$BR(b \rightarrow s\gamma) = (3.28 \pm 0.33) \times 10^{-4}. \quad (5.4)$$

The calculation of the width for $b \rightarrow s\gamma$ decay proceeds by calculating the loop interaction for $b \rightarrow s\gamma$ within a given model framework, *e.g.* the MSSM, at some high mass scale $Q \sim M_W$, and then matching to an effective theory Hamiltonian given by

$$H_{eff} = -\frac{4G_F}{\sqrt{2}} V_{tb} V_{ts}^* \sum_{i=1}^8 C_i(Q) O_i(Q), \quad (5.5)$$

where the $C_i(Q)$ are Wilson coefficients evaluated at scale Q , and the O_i are a complete set of operators relevant for the process $b \rightarrow s\gamma$ (given, for example, in Ref. [46].) All orders approximate QCD corrections are included via renormalization group resummation of leading logs (LL) which arise due to a disparity between the scale at which new physics enters the $b \rightarrow s\gamma$ loop corrections (usually taken to be $Q \sim M_W$), and the scale at which the $b \rightarrow s\gamma$ decay rate is evaluated ($Q \sim m_b$). Resummation then occurs when we solve the renormalization group equations (RGE's) for the Wilson coefficients

$$Q \frac{d}{dQ} C_i(Q) = \gamma_{ji} C_j(Q), \quad (5.6)$$

where γ is the 8×8 anomalous dimension matrix (ADM), and

$$\gamma = \frac{\alpha_s}{4\pi} \gamma^{(0)} + \left(\frac{\alpha_s}{4\pi}\right)^2 \gamma^{(1)} + \dots \quad (5.7)$$

The matrix elements of the operators O_i are finally calculated at a scale $Q \sim m_b$ and multiplied by the appropriately evolved Wilson coefficients to obtain the final decay amplitude.

Recently, next-to-leading order QCD corrections have been completed for $b \rightarrow s\gamma$ decay. These include *i)* complete virtual corrections [47] to the relevant operators O_2 , O_7 and O_8 which, when combined with bremsstrahlung corrections [48,47] results in cancellation of associated soft and collinear singularities; *ii)* calculation of $\mathcal{O}(\alpha_s^2)$ contributions to the ADM elements $\gamma_{ij}^{(1)}$ for $i, j = 1 - 6$ (by Ciuchini *et al.* [49]), for $i, j = 7, 8$ by Misiak and Münz [50], and for $\gamma_{27}^{(1)}$ by Chetyrkin, Misiak and Münz [51]. In addition, if two significantly different masses contribute to the loop amplitude, then there can already exist significant corrections to the Wilson coefficients at scale M_W . In this case, the procedure is to create a tower of effective theories with which to correctly implement the RG running between the multiple scales involved in the problem. The relevant operator bases, Wilson coefficients and RGEs are given by Cho and Grinstein [52] for the SM and by Anlauf [53] for the MSSM. The latter analysis includes contributions from just the tW , tH^- and $\tilde{t}_i \tilde{W}_j$ loops (which are the most important ones). We include the above set of QCD improvements (with the exception of $\gamma_{27}^{(1)}$, which has been shown to be small [51]) into our calculations of the $b \rightarrow s\gamma$ decay rate for the mSUGRA model.

We include the contributions to $C_7(M_W)$ and $C_8(M_W)$ from $\tilde{g}\tilde{q}$ and $\tilde{Z}_i\tilde{q}$ loops. To do so, the squark mixing matrix Γ which enters the couplings must be derived. To accomplish this, we first calculate the values of all running fermion masses in the SM at the mass scale M_Z . From these, we derive the corresponding Yukawa couplings f_u , f_d and h_e for each generation, and construct the corresponding Yukawa matrices $(f_u)_{ij}$, $(f_d)_{ij}$ and $(f_e)_{ij}$, where $i, j = 1, 2, 3$ runs over the 3 generations. We choose a basis that yields flavor diagonal matrices for $(f_d)_{ij}$ and $(f_e)_{ij}$, whereas the CKM mixing matrix creates a non-diagonal matrix $(f_u)_{ij}$ [27]. The three Yukawa matrices are evolved within the MSSM from $Q = M_Z$ up to $Q = M_{GUT}$ and the values are stored. At $Q = M_{GUT}$, the matrices $(A_u f_u)_{ij}$, $(A_d f_d)_{ij}$ and $(A_e f_e)_{ij}$ are constructed (assuming $A(M_{GUT}) = A_0 \times \mathbf{1}$). The squark and slepton mass squared matrices $(m_k^2)_{ij}$ are also constructed, where $k = \tilde{Q}, \tilde{u}, \tilde{d}, \tilde{L}$ and \tilde{e} . These matrices are assumed to be proportional to $\mathbf{1}$ at $Q = M_{GUT}$. The $(A f)_{ij}$ and $(m_k^2)_{ij}$ matrices are evolved along with the rest of the gauge/Yukawa couplings and soft SUSY breaking terms between M_Z and M_{GUT} iteratively via Runge-Kutta method until a stable solution is found. At $Q = M_Z$,

the 6×6 d -squark mass squared matrix is constructed. Numerical diagonalization of this matrix yields the squark mass mixing matrix Γ which is needed for computation of the $\tilde{g}\tilde{q}$ and $\tilde{Z}_i\tilde{q}$ loop contributions. At this point, the Wilson coefficients $C_7(M_W)$ and $C_8(M_W)$ can be calculated and evolved to $Q \sim m_b$ as described above, so that the $b \rightarrow s\gamma$ decay rate can be calculated [54,55].

As indicated above, the main non-SM contributions to $B(b \rightarrow s\gamma)$ are tH^\pm and $\tilde{t}_i\tilde{W}_j^\pm$. There is some correlation between the H^\pm and \tilde{t}_1 masses and the D-term mass parameter M_D , as we show in Fig. 8. Large values of the charged Higgs are guaranteed if $M_D > 350$ GeV, which involve also large values of the top squark mass. This is the most convenient situation for satisfying the experimental requirements for $B(b \rightarrow s\gamma)$, because the charged Higgs contribution decreases. Nevertheless, in order to decrease sufficiently the chargino contribution, it is necessary to work in a restricted region of parameter space, as indicated below. In contrast to the correlation in Fig. 8, there is no obvious correlation between the charged Higgs mass and the mass of the chargino.

Our results for the same parameter space planes as in Fig. 4 are shown in Fig. 9. Contours of $B(b \rightarrow s\gamma)$ are shown for $5, 6, 7, 8, 10$ and 15×10^{-4} . In frame *a*), for $A_0 = -m_{16}$, we see that very large values of $B(b \rightarrow s\gamma)$ are obtained, usually well above the CLEO 95% CL limit, except for the very largest values of $m_{1/2} \sim 1000$ GeV. In particular, the regions with the maximum rate for direct detection of dark matter also have $B(b \rightarrow s\gamma)$ values far in excess of experimental measurements. A similar behavior is seen in frame *b*) for $A_0 = 0$. The very large values of $B(b \rightarrow s\gamma)$ are typical of SUSY models with large values of $\tan\beta$ and $\mu < 0$. The qualitative behavior that Yukawa unification works best for the sign of μ which gives the largest values for $B(b \rightarrow s\gamma)$ has been noted previously by a number of authors [14,56].

We do note here that there may be other possible effects which could act to reduce the $b \rightarrow s\gamma$ branching fraction. Nontrivial flavor mixing in the down squark sector could result in significant non-cancelling contributions from gluino loop diagrams, thus reducing the value of $B(b \rightarrow s\gamma)$. Furthermore, additional sources of non-universality could act to yield values of $B(b \rightarrow s\gamma)$ more nearly in line with experimental values [56]. For instance, non-universality between generations is still allowed by $SO(10)$, and could lead to potentially large gluino loop contributions. This could, for instance, naturally be the case in a class of $SO(10)$ models where dynamics makes third generation sfermion masses much smaller than masses of other sfermions [57]. Also, modifications can occur by including large CP violating phases for terms such as the μ parameter which controls the alignment of the SM Wilson coefficients with the top squark contribution. Of course, such phases would also affect for instance the electron and neutron electric dipole moments, and even scattering cross sections [58]. Finally, radiative corrections due to Yukawa couplings are not included in the computation of the decay rate. Keeping these issues in mind, one should exercise judgement in drawing broad conclusions from the results of Fig. 9.

It is well known that the supersymmetric contribution to $B(b \rightarrow s\gamma)$ is proportional to $A_t\mu \tan\beta$ when $\tan\beta$ is large [59]. Motivated by this, we have made a dedicated search in a restricted area of parameter space of our specific model where A_t is close to zero at the weak scale. To be more specific, we consider:

$$\begin{aligned} 1300 \text{ GeV} &< m_{16} < 1700 \text{ GeV} \\ 1300 \text{ GeV} &< m_{10} < 1700 \text{ GeV} \end{aligned}$$

$$\begin{aligned}
300 \text{ GeV} &< M_D < 600 \text{ GeV} \\
50 \text{ GeV} &< m_{1/2} < 300 \text{ GeV} \\
800 \text{ GeV} &< A_0 < 1800 \text{ GeV}
\end{aligned}
\tag{5.8}$$

In Fig. 10, we plot the branching ratio $B(b \rightarrow s\gamma)$ as a function of the light chargino mass, including only the points that satisfy the experimental constraints from colliders (aside from the LEP2 chargino mass bound). We see that many solutions can occur with $B(b \rightarrow s\gamma)$ within the 95% CL range, and with a low value of $m_{1/2}$. These small A_t solutions typically have $m_{10} < m_{16}$, and very low chargino masses, but top squark masses above 1 TeV, which acts to suppress $\tilde{t}_i \tilde{W}_i$ loop contributions. They correspond to solutions mostly to the left of the diagonal line in the upper part of Fig. 1a).

B. Comparison with SO(10) analysis of Blazek and Raby

A recent study by Blazek and Raby has appeared [60] (BR), which also focusses on the rate for $b \rightarrow s\gamma$ decays in Yukawa unified $SO(10)$ models. There are a number of differences between their study and ours. The main difference is that BR, based on a global fit [61] of model 4c of Anderson *et al.* (Ref [4]), reject all models with $\mu < 0$ based on the generally large rate for $BR(b \rightarrow s\gamma)$ obtained. On the contrary, we reject all models with $\mu > 0$ based on the inability to achieve a high degree of Yukawa coupling unification. BR adopt a top-down solution to renormalization group running, and impose universality of all matter scalars at $Q = M_{GUT}$, although they allow for arbitrary GUT scale values of m_{H_u} and m_{H_d} , whose values are fixed by imposing REWSB. This allows BR to generate solutions with very small values of μ , so that their \tilde{Z}_1 will be largely Higgsino-like. They also generate rather small SUSY loop corrections to m_b , ranging from 0% – 8%. These may be in part due to the small values of $\alpha_s(M_Z)$ they generate, ranging from 0.11 – 0.18. In contrast, for $\mu > 0$, we generate SUSY loop corrections to m_b of order 10% – 40% at large $\tan\beta$, in accord with Pierce *et al.*, Ref. [22]. Using a bottom-up approach to renormalization group running, the large SUSY loop corrections to fermion masses allow us to generate Yukawa unification only good to 25% – 75% for this sign of μ (again in accord with Pierce *et al.*). Thus, if we allow a much more liberal constraint on Yukawa unification, we will also obtain $\mu > 0$ solutions, which in general can give $BR(b \rightarrow s\gamma)$ rates more closely in accord with measurements. We note that for $\mu > 0$, we find REWSB can occur for $\tan\beta \sim 50$, even assuming universality of *all* scalar masses (as mentioned earlier in Sec. I).

C. Note added:

After completion of this manuscript, a preprint appeared [62] wherein it was claimed that NLO corrections to the $b \rightarrow s\gamma$ loop diagrams [63,64] can lead to sign reversals on certain amplitudes, especially at large $\tan\beta$. This effect leads to rates for $b \rightarrow s\gamma$ decay in accord with theory predictions for Yukawa unified models with $\mu < 0$, while excluding models at large $\tan\beta$ with $\mu > 0$. In view of these (incomplete) calculations, it appears to us that one should view the restrictions from one-loop calculations of $b \rightarrow s\gamma$ decay with care. Rather than categorically excluding regions, it appears to be best to wait until complete

calculations are available. It would indeed be exciting if these corrections led to values of the $b \rightarrow s\gamma$ decay rate in agreement with experiment for the sign of μ favored by Yukawa unification.

VI. PROSPECTS FOR YUKAWA-UNIFIED $SO(10)$ AT THE FERMILAB TEVATRON

In Yukawa unified $SO(10)$ models, as with most SUSY models, the light Higgs boson is bounded by $m_h \lesssim 125$ GeV, and so may well be accessible to Tevatron searches with high luminosity and improved detectors [65,66,59]. The h boson will in general be difficult to distinguish from a SM Higgs boson, so that signatures from other sparticles or additional Higgs bosons would be useful. In much of the parameter space of Yukawa unified $SO(10)$ models, the gluinos, squarks and sleptons are too heavy to result in observable signals for the Fermilab Tevatron collider. There are, however, three exceptions to this. 1.) For low values of m_{16} , the pseudoscalar and heavy scalar Higgs bosons A and H may be accessible to searches via $p\bar{p} \rightarrow b\bar{b}A$ or $b\bar{b}H$. 2.) If $\tan\beta$ is on the lower end of acceptable values (*e.g.* $\tan\beta \sim 46 - 49$), then some regions of parameter space with low values of $m_{1/2}$ may be accessible to trilepton searches. 3.) For large negative values of the A_0 parameter, the \tilde{b}_1 -squark becomes light enough that there exists a substantial production cross section for $\tilde{b}_1\tilde{b}_1$ production. In this section, we address each of these possibilities.³

A. Search for the H and A Higgs bosons

Here, the search is for $b\bar{b}\phi$ events, where $\phi = A$ or H . At large $\tan\beta \sim 50$ as in Yukawa unified $SO(10)$, the $b\bar{b}A$ and $b\bar{b}H$ couplings are enhanced, leading to large production cross sections. For the Higgs mass range of interest, H and A typically decay to $b\bar{b}$ with a $\sim 90\%$ branching fraction, so that the signal will be four b -jet events, where two of the bs reconstruct to the Higgs mass. For Higgs masses in the range of interest, usually $m_H \sim m_A$, so that the resonances from each will be overlapping. The dominant backgrounds come from $b\bar{b}b\bar{b}$, $b\bar{b}jj$, $Wb\bar{b}$ and $Zb\bar{b}$ production.

In Fig. 11 we plot allowed regions in the m_{10} - m_A plane when the independent parameters of the theory are varied as indicated in Eq. (2.1). Four regions are displayed according to the value of the D-term mass parameter M_D (the four regions have a small overlap in their boundaries). The following correlation is obvious from the figure: a smaller CP-odd Higgs mass m_A is obtained for smaller M_D and m_{10} mass parameters. We have checked that the heaviest CP-even Higgs mass m_H is very close to m_A , in fact they are within $\pm 2\%$ ($\pm 5\%$) of each other for $m_A > 200$ (100) GeV. On the contrary, if m_A is decreased below 100 GeV, H becomes heavier than A , such that m_H can be up to 50% larger than m_A for $m_A \sim 80$.

³The effect of $SO(10)$ D -terms on SUSY cross sections at the Fermilab Tevatron collider has been examined in Ref. [67]. These authors do not insist on Yukawa unification, so that any value of $\tan\beta$ is allowed.

For the recently concluded year-long Tevatron workshop on SUSY/Higgs physics at Run 2, analyses have been performed to estimate the reach for H and A at large $\tan\beta$ for both the $D0$ and CDF detectors [28]. In this report, details of expected event rates, backgrounds and selection cuts can be found. For $\tan\beta = 50$, the 5σ discovery reach of the $D0$ detector is expected to be $m_A \simeq 145, 190$ and 220 GeV for integrated luminosities of 2, 10 and 30 fb^{-1} , respectively. Similarly, the reach of the CDF detector is estimated to be $m_A \simeq 130, 160$ and 220 GeV for the same integrated luminosities.

In Fig. 12, we show contours of m_A that correspond to the 5σ reach of the $D0$ detector, for the same parameter choices as in Fig. 4, assuming integrated luminosities of 2, 10 and 30 fb^{-1} . The region to the left of the contours ought to be accessible to Tevatron searches for $b\bar{b}H$ and $b\bar{b}A$ events. These regions represent the most likely possibility for detection of beyond the SM physics at the Tevatron if Yukawa unified $SO(10)$ is indeed correct.

B. Search for trilepton events

One of the most promising ways to detect supersymmetry at the Tevatron for models with universality and low values of $\tan\beta$ is via trilepton events, which dominantly come from $\tilde{W}_1\tilde{Z}_2 \rightarrow 3\ell + \cancel{E}_T$ [68]. At large values of $\tan\beta$ and low values for scalar masses, the branching fraction of \tilde{Z}_2 is dominated by real or virtual staus, so that the \tilde{Z}_2 branching fraction to e s or μ s is suppressed. Models with $m_{\tilde{W}_1} \lesssim 200$ GeV have the potential to yield significant trilepton signals at the Fermilab Tevatron $p\bar{p}$ collider.

In a recent paper [69], the trilepton signal at the Fermilab Tevatron was re-examined for the mSUGRA model, in light of new backgrounds from W^*Z^* and $W^*\gamma^*$ production and decay, and the inclusion of decay matrix elements into ISAJET. New sets of soft (SC2) and hard (HC2) cuts were proposed which allowed the trilepton signal to be seen at the Tevatron collider for integrated luminosities of 2 and 25 fb^{-1} . For the Yukawa unified $SO(10)$ model, we have used the background rates and the SC2 cuts presented in Ref. [69] to evaluate the observability of various points in model parameter space.

In scans of the parameter space corresponding to Fig. 4, no points were found where the Tevatron could see the 3ℓ signal using cuts SC2 with either 2 or 25 fb^{-1} of integrated luminosity. For both frames $a)$ and $b)$, the bottom squark \tilde{b}_1 is relatively light compared to other scalars so that \tilde{Z}_2 dominantly decays to $b\bar{b}\tilde{Z}_1$ final states, at the expense of e and μ modes.

By modifying the parameter space somewhat, it is possible to find significant regions where the 3ℓ signal should be visible. In Fig. 13, we show the m_{16} vs. $m_{1/2}$ plane for $m_{10} = 1.14m_{16}$, $A_0 = 0$, $\tan\beta = 47$ and $M_D = \frac{1}{3}m_{16}$. The mass contours shown are the same as in Fig. 2. In this case, there is a significant region below the $m_{\tilde{W}_1} = 150$ GeV contour accessible to Tevatron searches. No points were found to be observable at 5σ with just 2 fb^{-1} of integrated luminosity, using cuts SC2. However, the open squares denote points where a 5σ 3ℓ signal can be seen above background with 25 fb^{-1} . The diamonds denote points seeable at 3σ level with 25 fb^{-1} of data. In the region of parameter space with $m_{\tilde{W}_1} < 150$ GeV but with low values of m_{16} , the \tilde{b}_1 is becoming sufficiently light that three body \tilde{Z}_2 decays to b -quarks dominates. In the visible region at higher values of m_{16} , the squarks, including \tilde{b}_1 are so heavy that the \tilde{Z}_2 decay is dominated by the virtual Z contribution, and $\tilde{Z}_2 \rightarrow e^+e^-\tilde{Z}_1$ with typically a 3% branching fraction. If we use the same

parameters as in Fig. 13 but increase $\tan\beta$ to 50, then the \tilde{b}_1 becomes so light that again \tilde{Z}_2 dominantly decays to b -quarks, and the trilepton signal vanishes.

C. Search for direct production of b -squarks

In the Yukawa unified $SO(10)$ model, it has been noted in Ref. [21] that a combination of the large b -quark Yukawa coupling plus the D -term contribution to the \tilde{b}_R squared mass yields parameter ranges with the light b -squark \tilde{b}_1 being by far the lightest of all the squarks. In fact, frequently \tilde{b}_1 is also much lighter than all the sleptons. This means that there may be regions of model parameter space where $\tilde{b}_1\tilde{\bar{b}}_1$ pairs can be produced at large rates, with possibly observable signals.

In Fig. 14 we show the lightest bottom squark mass $m_{\tilde{b}_1}$ as a function of m_{16} for different values of the D -term parameter M_D . The three regions correspond to $M_D < 220$ GeV, $220 \text{ GeV} < M_D < 330$ GeV, and $330 < M_D$ GeV, with some overlap at the boundaries. The smallest bottom squark masses we obtain satisfy $m_{\tilde{b}_1} < 200$ GeV and occur for intermediate values of M_D and m_{16} . These points have approximately $\mu \sim -200$ GeV imposed by EWSB (and $A_0 \sim -1600$ GeV). This value of μ together with the large value of $\tan\beta$, makes the left-right sbottom mixing comparable with the right sbottom soft mass parameter m_D .

In Ref. [29], the reach of the Tevatron collider for $\tilde{b}_1\tilde{\bar{b}}_1$ pairs was investigated. If $\tilde{b}_1 \rightarrow b\tilde{Z}_1$ is the dominant decay mode, then the final state will include two hard b -jets plus E_T . Backgrounds investigated included $W+jets$, $Z+jets$ and $t\bar{t}$ production. For the vector boson production backgrounds, the *jets* qualifier includes both b -jets and other light quark jets. A number of cuts were proposed, including tagging the b -jets via microvertex detectors, which allowed signals to be seen above backgrounds in large parts of the $m_{\tilde{b}_1}$ vs. $m_{\tilde{Z}_1}$ parameter space. Typically, bottom squark masses of $m_{\tilde{b}_1} \simeq 210$ GeV could be seen with 2 fb^{-1} , and $m_{\tilde{b}_1} \simeq 240$ GeV could be seen with 25 fb^{-1} . The reach was somewhat reduced if $\tilde{b}_1 \rightarrow b\tilde{Z}_2$ decays were also kinematically accessible.

In Fig. 15, we show the same parameter space as in Fig. 4a). We have generated events with ISAJET for $p\bar{p}$ collisions at $\sqrt{s} = 2$ TeV using the detector simulation, cuts and background rates described in Ref. [29]. Parameter space points labelled with a star are seeable at the 5σ level with just 2 fb^{-1} of integrated luminosity. In addition, points labelled with an open square are seeable at 25 fb^{-1} . The open squares have \tilde{b}_1 masses as heavy as 245 GeV.

VII. SUMMARY, CONCLUSIONS AND OUTLOOK

We have shown before that supersymmetric particle spectra can be calculated in minimal supersymmetric $SO(10)$ GUT models consistent with Yukawa coupling unification to 5% or better, a top mass of $m_t = 175$ GeV and including radiative electroweak symmetry breaking. To accomplish this, we made crucial use of D -term contributions to scalar masses that are induced by the reduction in rank of gauge symmetry when $SO(10)$ breaks to the MSSM at $Q = M_{GUT}$. The D -terms split the GUT scale values of the Higgs boson squared masses so that $m_{H_u}^2 < m_{H_d}^2$ already at M_{GUT} . This allows $m_{H_u}^2$ to be driven more negative than $m_{H_d}^2$ at $Q = M_{weak}$, which is required for REWSB to take place. We included the essential SUSY

loop corrections to third generation fermion masses to generate the appropriate weak scale Yukawa couplings. Yukawa unification to 5% takes place only for $\mu < 0$ and $\tan\beta \sim 46 - 52$. In this paper, we upgraded our Yukawa coupling evolution equations to include two-loop terms in the RGEs plus weak-scale threshold effects for the one-loop terms.

The sparticle mass spectra we calculate reflect the influence of the D -terms, and as a consequence, the \tilde{b}_1 turns out to be almost always the lightest of the squarks, and is sometimes even lighter than the sleptons. In addition, the lightest sleptons can frequently be (dominantly) left- sparticles, as opposed to the mSUGRA model where they are usually right- sparticles. This latter trait may be tested explicitly at e^+e^- linear colliders operating above slepton pair production threshold.

We attempted to systematize the parameter space of these models, showing plots of sparticle mass in the m_{16} *vs.* $m_{1/2}$ plane for viable selections of m_{10} , M_D and $\tan\beta$. Of course, fixing these parameters meant we had to loosen our restrictions on the degree of Yukawa coupling unification. We stress though that the original degree of unification can be regained by a small change in $\tan\beta$.

We calculated the relic density of neutralinos in Yukawa unified $SO(10)$, and found none of the parameter space that was explored to be excluded by the limits on the age of the universe. In fact, very desirable values for $\Omega_{\tilde{Z}_1} h^2$ were found throughout much of parameter space.

We also evaluated the direct neutralino detection rate for a ^{73}Ge detector. Detection rates could exceed 1 event/kg/day, but only in parameter regions with very low relic densities. In more favorable regions, the direct detection rate often exceeded 0.01 events/kg/day, which is the capability being sought by current generation dark matter detection experiments.

We also examined the branching ratio for $b \rightarrow s\gamma$ decay in Yukawa unified $SO(10)$. We found that it was beyond the 95%CL experimental limits for much of the parameter space shown. However, special regions of parameter space giving rise to small values of weak scale A_t gave more acceptable $B(b \rightarrow s\gamma)$ values, but with $m_{\tilde{t}_1} \geq 1$ TeV. There could be other mechanisms such as non-trivial mixing in the squark sector, additional non-universality or mixing, or CP violating phases could act to reduce the large $B(b \rightarrow s\gamma)$ values. Alternatively, the rate for $b \rightarrow s\gamma$ is more favorable for $\mu > 0$, but then the degree of Yukawa unification would have to be relaxed substantially. Finally, recent claims have been made [62] that two-loop $b \rightarrow s\gamma$ calculations can actually reverse the signs of certain decay amplitudes, leading to the possibility of agreement between $b \rightarrow s\gamma$ calculations and Yukawa unified SUSY models with $\mu < 0$. In light of these claims, it seems prudent to refrain from excluding parameter space regions based on one-loop $b \rightarrow s\gamma$ calculations until the theoretical predictions become more certain.

We found three possibilities for new particle detection at the upgraded Fermilab Tevatron beyond discovery of the lightest Higgs boson. In regions of parameter space with small m_{16} , $b\bar{b}A$ and $b\bar{b}H$ production could be visible. In some parameter space regions with small $m_{1/2}$, it is possible to detect trilepton signals from $\tilde{W}_1\tilde{Z}_2 \rightarrow 3\ell$ production. In other regions again with small $m_{1/2}$, bottom squark pair production may yield a visible signal. The other scalar particles are generally too heavy to be produced substantially at the Tevatron collider.

At the LHC, we expect Yukawa unified $SO(10)$ to be visible as usual for values of $m_{\tilde{g}}$ beyond ~ 2 TeV. Within this framework, SUSY events ought to be rich in b -quark jets due to the relatively light third generation squark masses inherent in this theory.

Yukawa unified $SO(10)$ models have been historically very compelling models for reasons listed in the introduction, and are even more compelling today due to recent strong evidence on neutrino masses. The Yukawa unified $SO(10)$ model is only one of a number of $SO(10)$ models that are possible. A more general $SO(10)$ model [24] could contain a superpotential with terms such as

$$\hat{f} = f_b \hat{\psi} \hat{\psi} \hat{\phi}_d + f_t \hat{\psi} \hat{\psi} \hat{\phi}_u + \dots \quad (7.1)$$

in which case just $b - \tau$ unification would occur. This would allow a much wider range of $\tan \beta \sim 30 - 50$ to occur [24].

In addition, recent work on radiatively driven inverted hierarchy models has shown that “natural” models can be obtained with multi-TeV scale scalar masses, where the third generation masses are driven to weak scale values [70]. These models suffer the same problem with REWSB (and possible color and charge breaking minima in the scalar potential) as the $SO(10)$ model considered here. It has recently been shown that D -term contributions to scalar masses aid this class of models to achieve REWSB [57]. Finally, more complex gauge symmetry breaking patterns could occur which would affect scalar masses in alternative ways [71].

ACKNOWLEDGMENTS

We thank Diego Castaño, Damien Pierce and Konstantin Matchev for discussions. This research was supported in part by the U. S. Department of Energy under contract numbers DE-FG02-97ER41022 and DE-FG03-94ER40833. M.A.D. was supported in part by CONICYT-1000539.

REFERENCES

- [1] H. Georgi, in *Proceedings of the American Institute of Physics*, edited by C. Carlson (1974); H. Fritzsch and P. Minkowski, *Ann. Phys.* **93**, 193 (1975); M. Gell-Mann, P. Ramond and R. Slansky, *Rev. Mod. Phys.* **50**, 721 (1978); for a review of SUSY $SO(10)$, see R. Mohapatra, hep-ph/9911272 (1999).
- [2] J. Lykken, T. Montroy and S. Willenbrock, *Phys. Lett.* **B418**, 141 (1998).
- [3] M. Gell-Mann, P. Ramond and R. Slansky, in *Supergravity, Proceedings of the Workshop*, Stony Brook, NY 1979 (North-Holland, Amsterdam); T. Yanagida, KEK Report No. 79-18, 1979; R. Mohapatra and G. Senjanovic, *Phys. Rev. Lett.* **44**, 912 (1980).
- [4] Some references include S. Dimopoulos, L. Hall and S. Raby, *Phys. Rev. Lett.* **68**, 1984 (1992) and *Phys. Rev. D* **46**, 4793 (1992); G. Anderson, S. Raby, S. Dimopoulos, L. Hall and G. Starkman, *Phys. Rev. D* **49**, 3660 (1994); M. Carena, S. Dimopoulos, C. Wagner and S. Raby, *Phys. Rev. D* **52**, 4133 (1995); K. Babu and S. Barr, *Phys. Rev. D* **56**, 2614 (1997); K. Babu, J. Pati and F. Wilczek, *Nucl. Phys.* **B566**, 33 (2000); C. Albright and S. Barr, *Phys. Rev. D* **58**, 013002 (1998).
- [5] L. Hall and M. Suzuki, *Nucl. Phys.* **B231**, 419 (1984); R. Mohapatra, *Phys. Rev. D* **34**, 3457 (1986); A. Font, L. Ibanez and F. Quevedo, *Phys. Lett.* **B228**, 79 (1989).
- [6] S. P. Martin, *Phys. Rev. D* **46**, 2769 (1992) and *Phys. Rev. D* **54**, 2340 (1996).
- [7] C. Aulakh, A. Melfo, A. Rasin and G. Senjanovic, *Phys. Lett.* **B459**, 557 (1999).
- [8] M. Fukugita and T. Yanagida, *Phys. Lett.* **B174**, 45 (1986); T. Gherghetta and G. Jungman, *Phys. Rev. D* **48**, 1546 (1993); W. Buchmuller and M. Plumacher, *Phys. Lett.* **B389**, 73 (1996); T. Moroi and H. Murayama, hep-ph/9908223 (1999).
- [9] See for instance K. Babu and S. Barr, *Phys. Rev. D* **51**, 2463 (1995); S.M. Barr and S. Raby, *Phys. Rev. Lett.* **79**, 4748 (1997); L. Hall and S. Raby, *Phys. Rev. D* **51**, 6524 (1995); C. Albright and S. M. Barr, hep-ph/0003251 (2000).
- [10] M. Olechowski and S. Pokorski, *Nucl. Phys.* **B404**, 590 (1993).
- [11] V. Barger, M. Berger and P. Ohmann, *Phys. Rev. D* **49**, 4908 (1994).
- [12] M. Carena, M. Olechowski, S. Pokorski and C. Wagner, *Nucl. Phys.* **B426**, 269 (1994).
- [13] B. Ananthanarayan, Q. Shafi and X. Wang, *Phys. Rev. D* **50**, 5980 (1994); B. Ananthanarayan, G. Lazarides and Q. Shafi, *Phys. Lett.* **B300**, 245 (1993).
- [14] M. Carena and C. Wagner, CERN-TH-7321-94 (1994).
- [15] L. J. Hall, R. Rattazzi and U. Sarid, *Phys. Rev. D* **50**, 7048 (1994); R. Rattazzi, U. Sarid and L. Hall, hep-ph/9405313 (1994); R. Rattazzi and U. Sarid, *Phys. Rev. D* **53**, 1553 (1996).
- [16] D. Matalliotakis and H. Nilles, *Nucl. Phys.* **B435**, 115 (1995).
- [17] R. Hempfling, *Phys. Rev. D* **52**, 4106 (1995).
- [18] P. Ciafaloni, A. Romanino and A. Strumia, *Nucl. Phys.* **B458**, 3 (1996).
- [19] M. Olechowski and S. Pokorski, *Phys. Lett.* **B344**, 201 (1995).
- [20] R. Rattazzi and U. Sarid, Ref. [15]; H. Murayama, M. Olechowski and S. Pokorski, *Phys. Lett.* **B371**, 57 (1996).
- [21] H. Baer, M. Diaz, J. Ferrandis and X. Tata, *Phys. Rev. D* **61**, 111701 (2000).
- [22] D. Pierce, J. Bagger, K. Matchev and R. Zhang, *Nucl. Phys.* **B491**, 3 (1997).
- [23] M. Drees, *Phys. Lett.* **B181**, 279 (1986); J.S. Hagelin and S. Kelley, *Nucl. Phys.* **B342**, 95 (1990); A.E. Faraggi, *et al.*, *Phys. Rev. D* **45**, 3272 (1992); Y. Kawamura and M. Tanaka, *Prog. Theor. Phys.* **91**, 949 (1994); Y. Kawamura, *et al.*, *Phys. Lett.* **B324**, 52 (1994);

- Phys. Rev. D**51**, 1337 (1995); N. Polonsky and A. Pomarol, Phys. Rev. D**51**, 6532 (1994); H.-C. Cheng and L.J. Hall, Phys. Rev. D**51**, 5289 (1995); C. Kolda and S.P. Martin, Phys. Rev. D**53**, 3871 (1996).
- [24] H. Baer, M. Diaz, P. Quintana and X. Tata, JHEP **0004**, 016 (2000).
 - [25] F. Paige, S. Protopopescu, H. Baer and X. Tata, hep-ph/0001086 (2000).
 - [26] V. Barger, M. Berger and P. Ohmann, Phys. Rev. D**47**, 1093 (1993).
 - [27] D. Castano, E. Piard and P. Ramond, Phys. Rev. D**49**, 4882 (1994).
 - [28] M. Roco, A. Belyaev and J. Valls, contribution to the Report of the Higgs working group to the Fermilab Workshop on Higgs/SUSY at Run2.
 - [29] H. Baer, P. Mercadante and X. Tata, Phys. Rev. D**59**, 015010 (1999); see also, R. Demina, J. Lykken, K. Matchev and A. Nomerotski, hep-ph/9910275 (1999).
 - [30] For a review, see M. Turner, astro-ph/9904051 (1999).
 - [31] M. Drees and M. Nojiri, Phys. Rev. D**47**, 376 (1993).
 - [32] H. Baer and M. Brhlik, Phys. Rev. D**53**, 597 (1996).
 - [33] P. Gondolo and G. Gelmini, Nucl. Phys. B**360**, 145 (1991).
 - [34] J. Ellis, T. Falk, K. Olive and M. Srednicki, Astropart. Phys. **13**, 181 (2000).
 - [35] See M. E. Gomez, G. Lazarides and C. Pallis, hep-ph/9907261 (1999) and hep-ph/0004028 (2000).
 - [36] C. Boehm, A. Djouadi and M. Drees, hep-ph/9911496 (1999) have pointed out the significance of a top squark roughly degenerate with the lightest neutralino for the computation of the relic density.
 - [37] For a review of dark matter detectors, see *e.g.* J. R. Primack, B. Sadoulet and D. Seckel, Ann. Rev. Nucl. Part. Sci. **B38**, 751 (1988); P. F. Smith and J. D. Lewin, Phys. Rep. **187**, 203 (1990); D. Cline, UCLA-APH-0096-3-97 (1997); L. Baudis *et al.* (GENIUS Collaboration), hep-ph/9910205 (1999).
 - [38] H. Baer and M. Brhlik, Phys. Rev. D**57**, 567 (1998).
 - [39] R. A. Flores, Phys. Lett. B**215**, 73 (1988); see also M. S. Turner, Phys. Rev. D**33**, 899 (1986) and E. Gates, G. Gyuk and M. Turner, FERMILAB-Pub-95/090-A (1995), astro-ph/9505039.
 - [40] M. Drees and M. Nojiri, Phys. Rev. D**47**, 4226 (1993) and Phys. Rev. D**48**, 3483 (1993).
 - [41] S. Bertolini, F. Borzumati, A. Masiero and G. Ridolfi, Nucl. Phys. B**353**, 591 (1991).
 - [42] R. Barbieri and G.F. Giudice, Phys. Lett. B **309**, 86 (1993); N. Oshimo, Nucl. Phys. B**404**, 20 (1993); M.A. Díaz, Phys. Lett. B **304**, 278 (1993), and Phys. Lett. B **322**, 207 (1994); J.L. Lopez, D.V. Nanopoulos, and G.T. Park, Phys. Rev. D **48**, 974 (1993); Y. Okada, Phys. Lett. B **315**, 119 (1993); R. Garisto and J.N. Ng, Phys. Lett. B **315**, 372 (1993); V. Barger *et al.* Phys. Rev. D**51**, 2438 (1995).
 - [43] R. Barate *et al.* (ALEPH Collaboration), Phys. Lett. B**429**, 169 (1998).
 - [44] S. Ahmed *et al.* (CLEO Collaboration), hep-ex/9908022 (1999).
 - [45] Ref. [51], A. Buras, A. Kwiatkowski and N. Pott, Phys. Lett. B**414**, 157 (1997); *ibid.*, erratum, Phys. Lett. B**434**, 459 (1998); and C. Grueb and T. Hurth, hep-ph/9708214 (1997).
 - [46] See, *e.g.*, B. Grinstein, M. J. Savage and M. Wise, Nucl. Phys. B**319**, 271 (1989); A. Ali, in *20th International Nathiagali Summer College on Physics and Contemporary Needs*, Bhurban, Pakistan, 1995, hep-ph/9606324.
 - [47] C. Greub, T. Hurth and D. Wyler, Phys. Lett. B**380**, 385 (1996) and Phys. Rev. D**54**,

- 3350 (1996).
- [48] A. Ali and C. Greub, Z. Phys. **C49**, 431 (1991), Phys. Lett. **B259**, 182 (1991), **287**, 191 (1992) and **361**, 146 (1995); Z. Phys. **C60**, 433 (1993); N. Pott, Phys. Rev. **D54**, 938 (1996).
 - [49] M. Ciuchini, E. Franco, G. Martinelli and L. Reina, Nucl. Phys. **B415**, 403 (1994).
 - [50] M. Misiak and M. Münz, Phys. Lett. **B344**, 308 (1995).
 - [51] K. G. Chetyrkin, M. Misiak and M. Münz, Phys. Lett. **B400**, 206 (1997).
 - [52] P. Cho and B. Grinstein, Nucl. Phys. **B365**, 279 (1991).
 - [53] H. Anlauf, Nucl. Phys. **B430**, 245 (1994).
 - [54] H. Baer and M. Brhlik, Phys. Rev. **D55**, 3201 (1997).
 - [55] H. Baer, M. Brhlik, D. Castano and X. Tata, Phys. Rev. **D58**, 015007 (1998).
 - [56] F. Borzumati, M. Olechowski and S. Pokorski, Phys. Lett. **B349**, 311 (1995).
 - [57] H. Baer, P. Mercadante and X. Tata, Phys. Lett. **B475**, 289 (2000).
 - [58] M. Brhlik and G. Kane, Phys. Lett. **B437**, 331 (1998).
 - [59] M. Carena, S. Mrenna and C. Wagner, Phys. Rev. **D60**, 075010 (1999).
 - [60] T. Blazek and S. Raby, Phys. Rev. **D59**, 095002 (1999).
 - [61] T. Blazek, M. Carena, S. Raby and C. Wagner, Phys. Rev. **D56**, 6919 (1997).
 - [62] W. de Boer, M. Huber, A. V. Gladyshev and D. I. Kazakov, hep-ph/0007078 (2000).
 - [63] M. Ciuchini, G. Degrassi, P. Gambino and G. F. Giudice, Nucl. Phys. **B534**, 3 (1998).
 - [64] C. Bobeth, M. Misiak and J. Urban, hep-ph/9904413 (1999).
 - [65] J. Conway, talk at SUSY99, Fermilab, June, 1999.
 - [66] H. Baer, B. Harris and X. Tata, Phys. Rev. **D59**, 015003 (1999).
 - [67] A. Datta, A. Datta, M. Drees and D. P. Roy, Phys. Rev. **D61**, 055003 (2000).
 - [68] For recent work, see H. Baer, M. Drees, F. Paige, P. Quintana and X. Tata, Phys. Rev. **D61**, 095007 (2000); V. Barger and C. Kao, Phys. Rev. **D60**, 115015 (1999); K. Matchev and D. Pierce, Phys. Rev. **D60**, 075004 (1999) and Phys. Lett. **B467**, 225 (1999); see also, S. Abel *et al.*, hep-ph/0003154 (2000).
 - [69] See H. Baer *et al.*, Ref. [68].
 - [70] J. Feng, C. Kolda and N. Polonsky, Nucl. Phys. **B546**, 3 (1999); J. Bagger, J. Feng and N. Polonsky, Nucl. Phys. **B563**, 3 (1999); J. Bagger, J. Feng, N. Polonsky and R. Zhang, Phys. Lett. **B473**, 264 (2000).
 - [71] See Y. Kawamura, H. Murayama and M. Yamaguchi, Ref. [23].

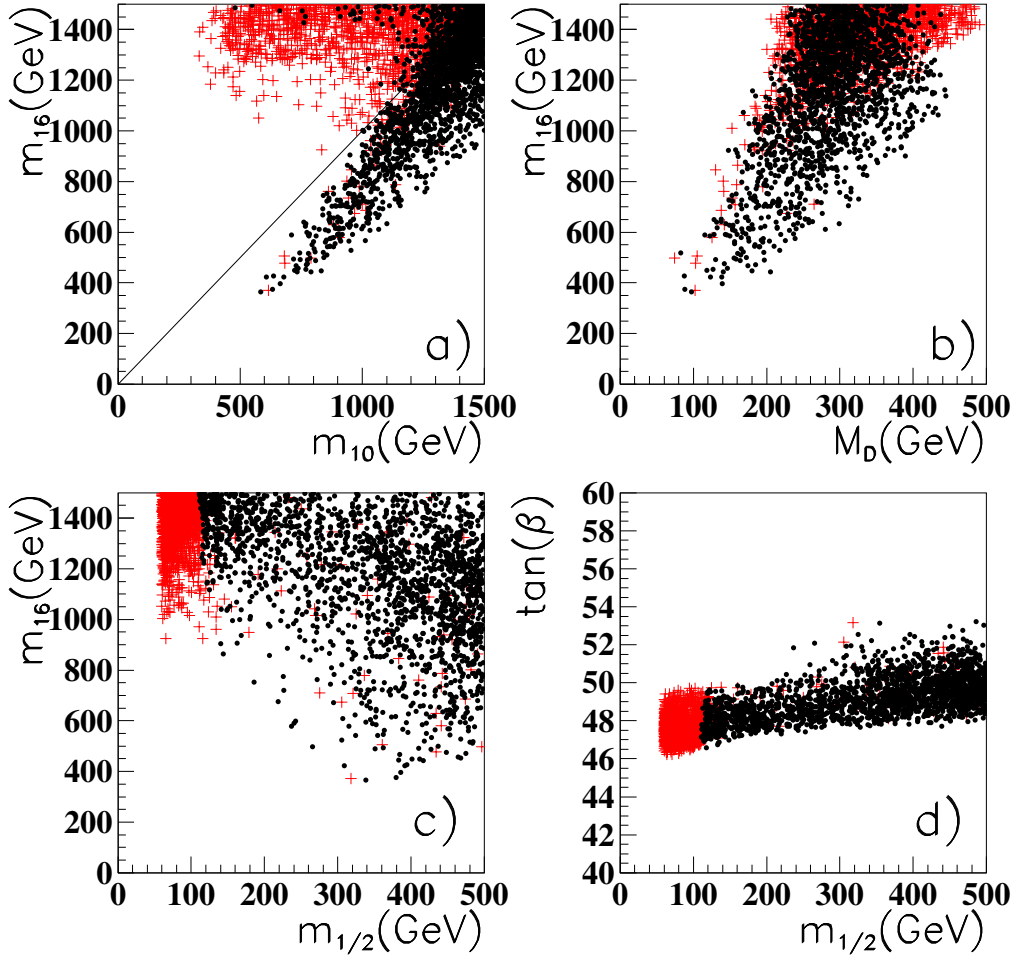


FIG. 1. Plots of regions of parameter space where valid solutions to minimal SUSY $SO(10)$ are obtained, consistent with Yukawa coupling unification to 5%, and radiative electroweak symmetry breaking. We use 2-loop RGEs for both gauge and Yukawa coupling evolution.

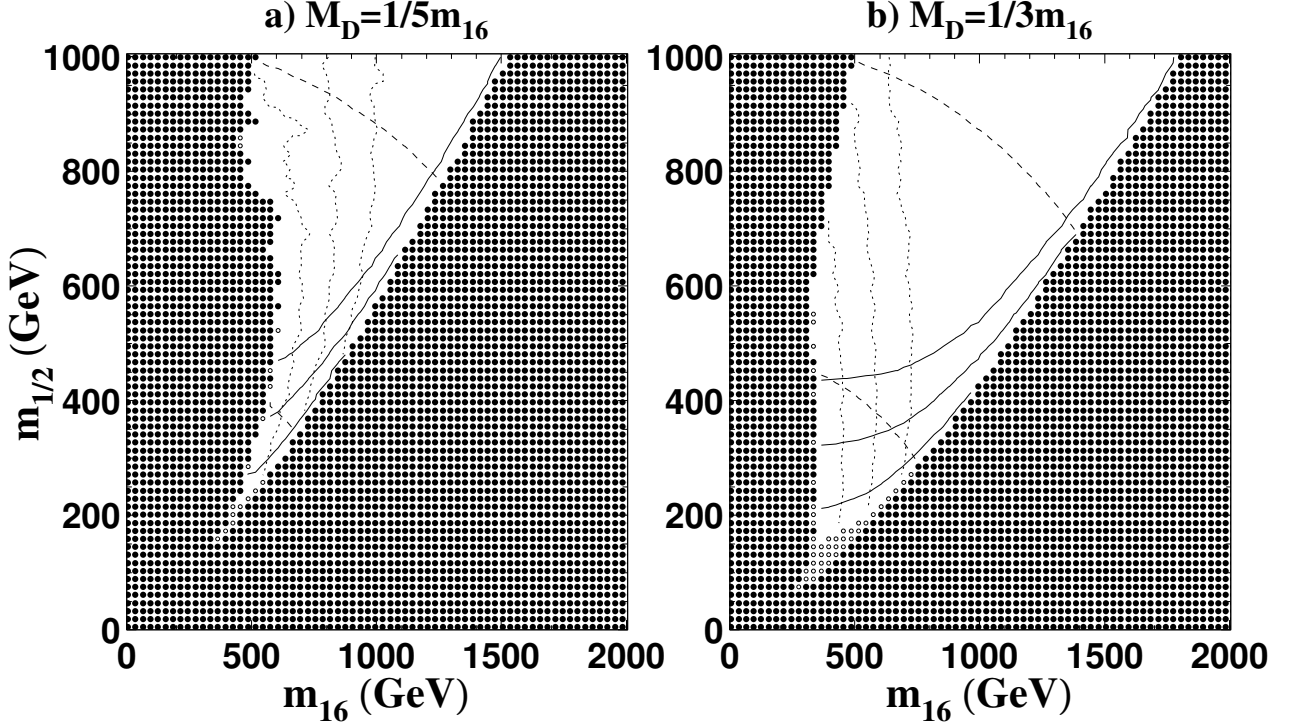


FIG. 2. We plot theoretically allowed regions of m_{16} vs. $m_{1/2}$ parameter space taking $A_0 = 0$, $m_{10} = 1.25m_{16}$, $\tan\beta = 50$ and $\mu < 0$. In frame a) we take $M_D = \frac{1}{5}m_{16}$, while frame b) we take $M_D = \frac{1}{3}m_{16}$. The shaded areas are not allowed by the REWSB constraint. Open dots represent experimentally excluded points. The dashed contours, from bottom to top, are for $m_{\tilde{u}_L} = 1000$ and 2000 GeV. The solid contours, from bottom to top, represent $m_{\tilde{W}_1}$ masses of 150, 250 and 350 GeV. The dotted contours represent from left to right $m_A = 150, 250$ and 350 GeV. Yukawa coupling unification varies from less than 5% in the central regions of the plot, to nearly 25% at the edges of the excluded region.

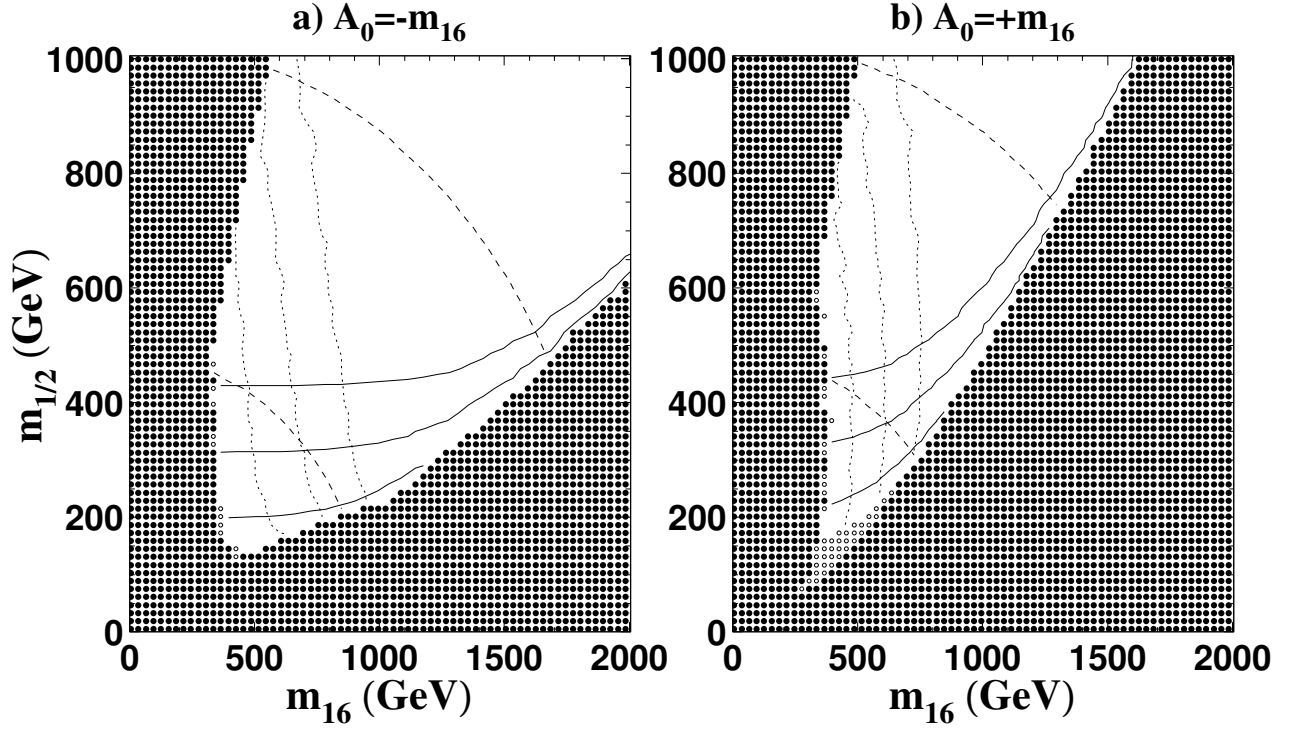


FIG. 3. The same as Fig. 2, except $M_D = \frac{1}{3}m_{16}$, while in *a*), $A_0 = -m_{16}$ and in *b*), $A_0 = +m_{16}$.

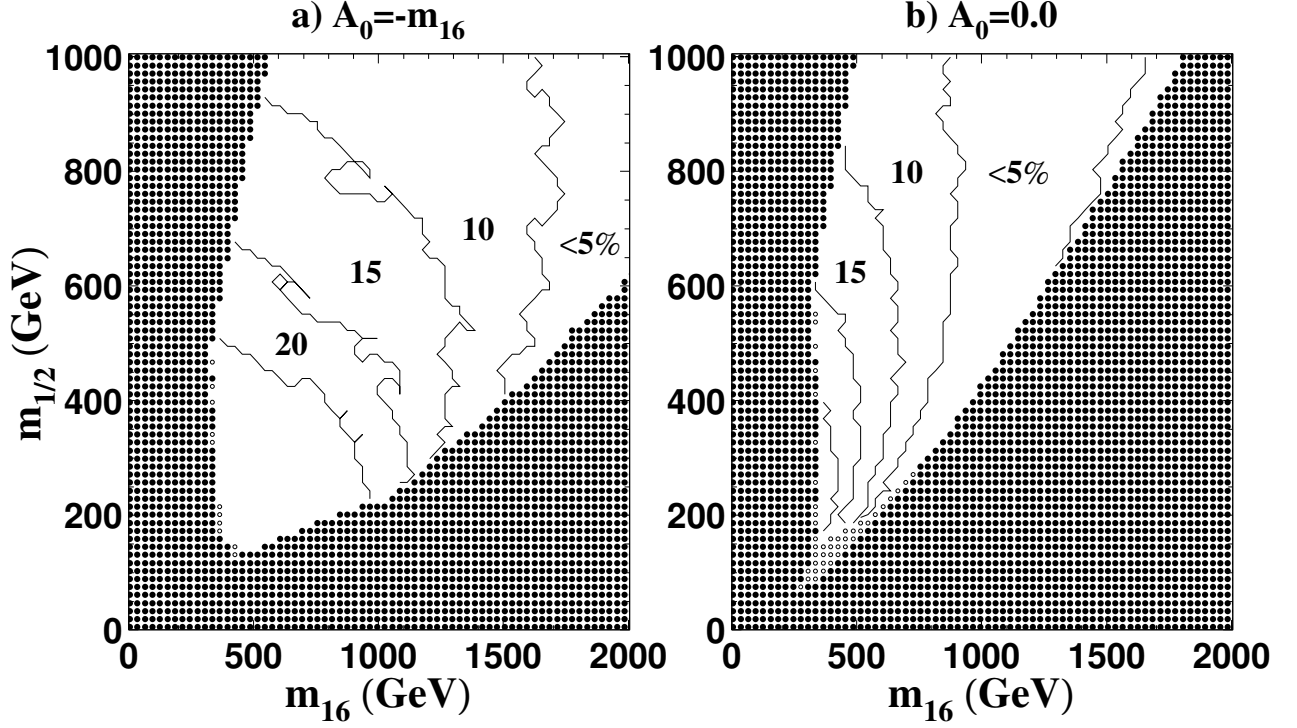


FIG. 4. Contours showing Yukawa coupling unification in the m_{16} vs. $m_{1/2}$ plane, for $M_D = \frac{1}{3}m_{16}$, $\tan \beta = 50$, $m_{10} = 1.25m_{16}$, $\mu < 0$ and a) $A_0 = -m_{16}$ and b) $A_0 = 0$. In frame b) the degree of unification reduces to 5-10% beyond the right-most contour in the figure.

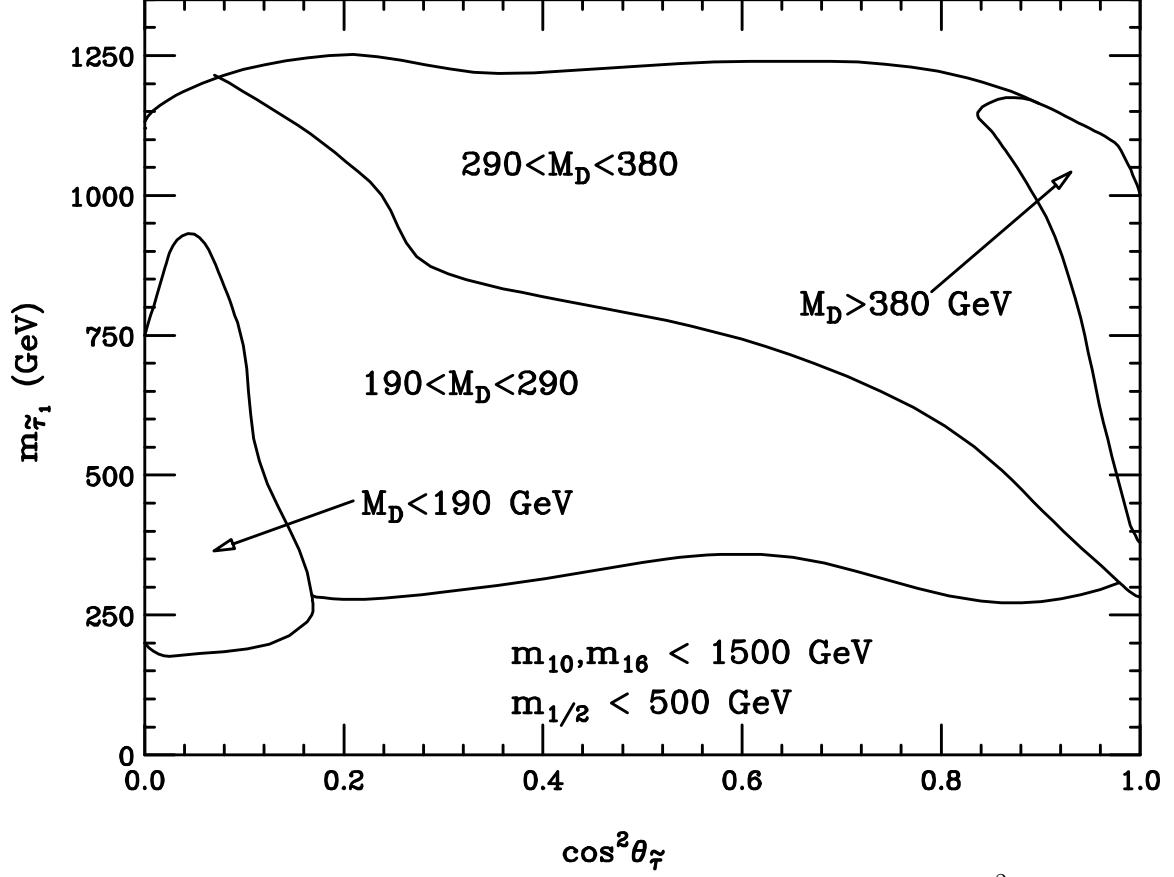


FIG. 5. Lightest stau mass as a function of the stau mixing parameter $\cos^2 \theta_{\tilde{\tau}}$ for different values of the D-term parameter M_D . In $SO(10)$ the stau mixing can take any value.

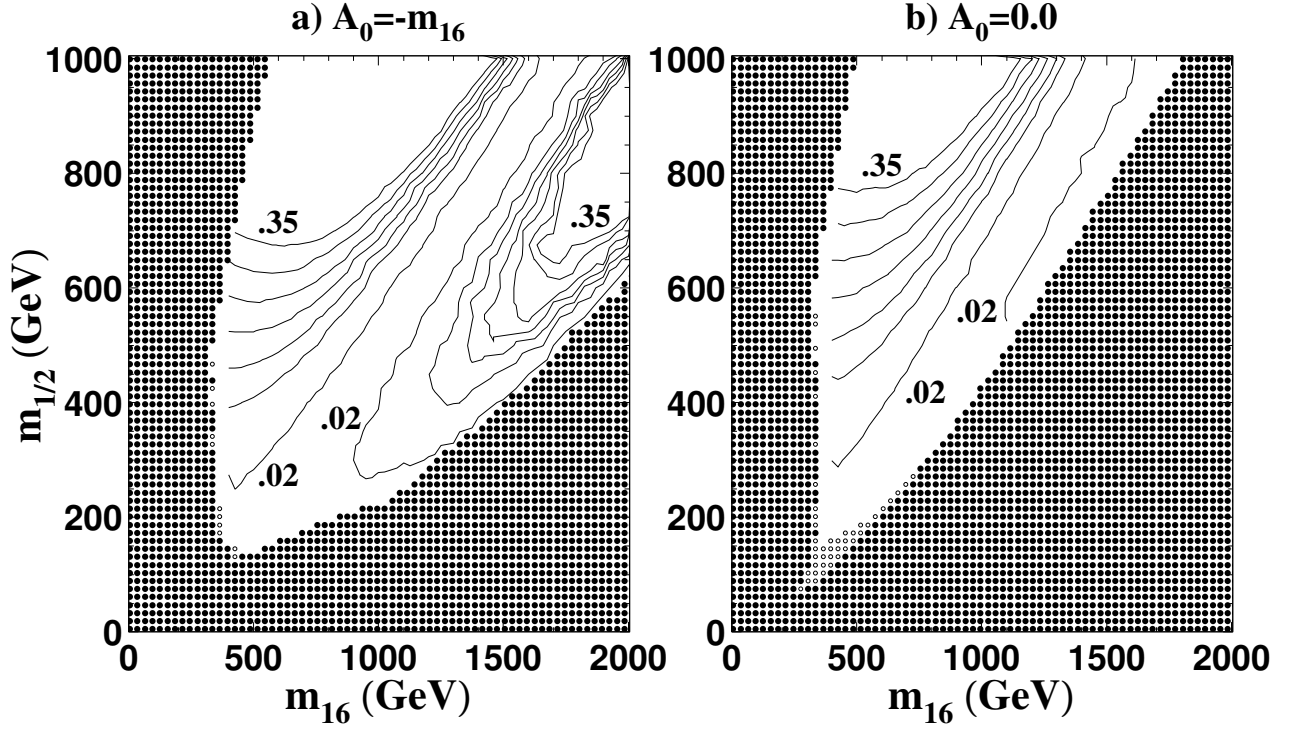


FIG. 6. The same parameter space planes as in Fig. 4, but now showing contours of neutralino relic density $\Omega_{\tilde{Z}_1} h^2 = 0.02, 0.1, 0.15, 0.2, 0.25, 0.30$ and 0.35 .

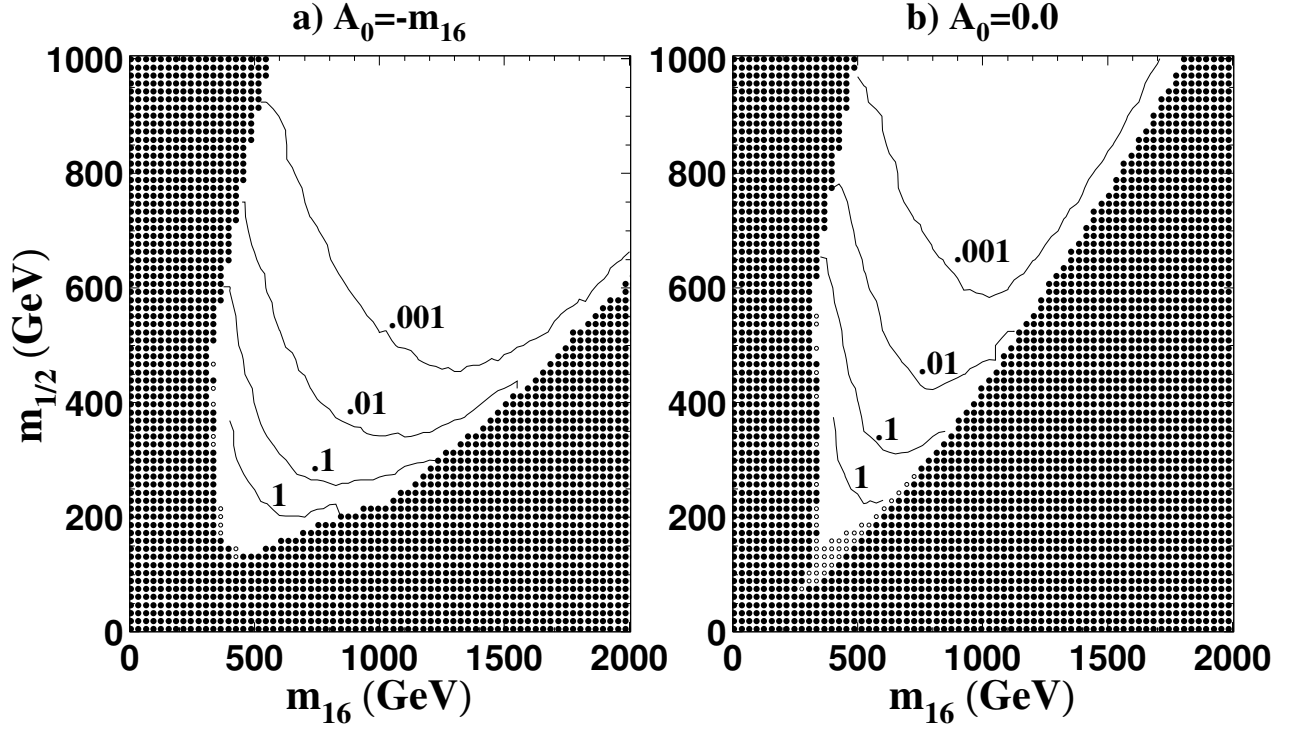


FIG. 7. The same parameter space planes as in Fig. 4, but now showing contours of direct neutralino detection rate in events/kg/day in a ^{73}Ge detector.

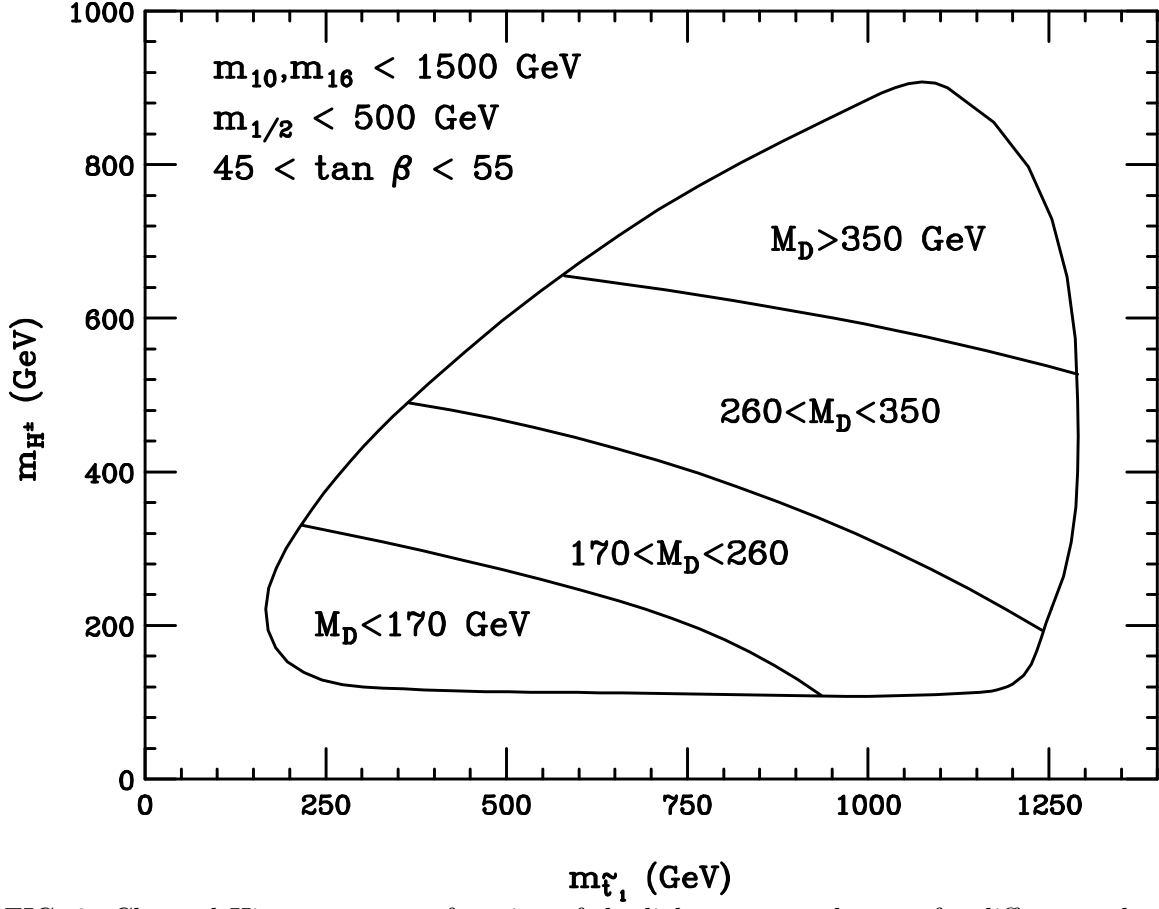


FIG. 8. Charged Higgs mass as a function of the light top squark mass for different values of the D-term parameter M_D . Heavy H^\pm and \tilde{t}_1 are associated with large values of M_D , which is favoured by $B(b \rightarrow s\gamma)$. Here, $\mu < 0$ and $|A_0| < 3 \text{ TeV}$.

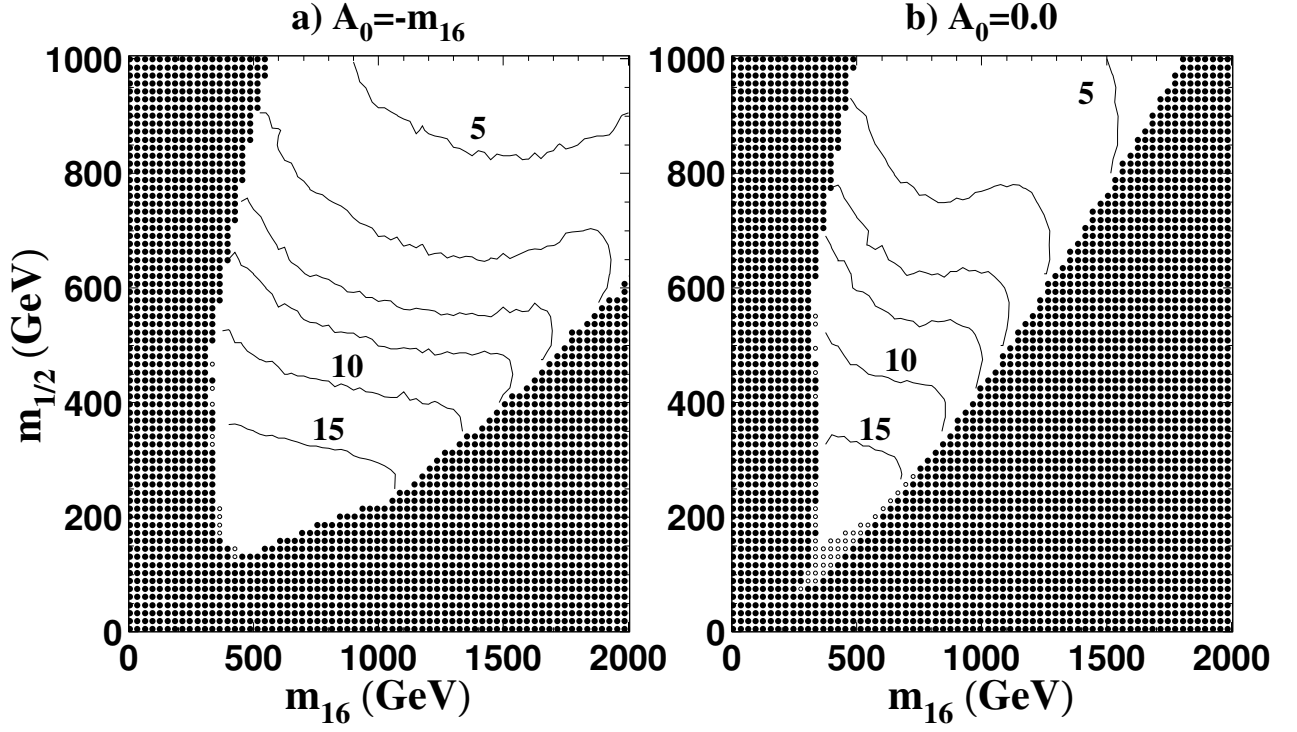


FIG. 9. The same parameter space planes as in Fig. 4, but now showing contours of decay branching fraction for $b \rightarrow s\gamma$. Starting from the top, the contours are for a branching fraction of 5, 6, 7, 8, 10 and 15 times 10^{-4} .

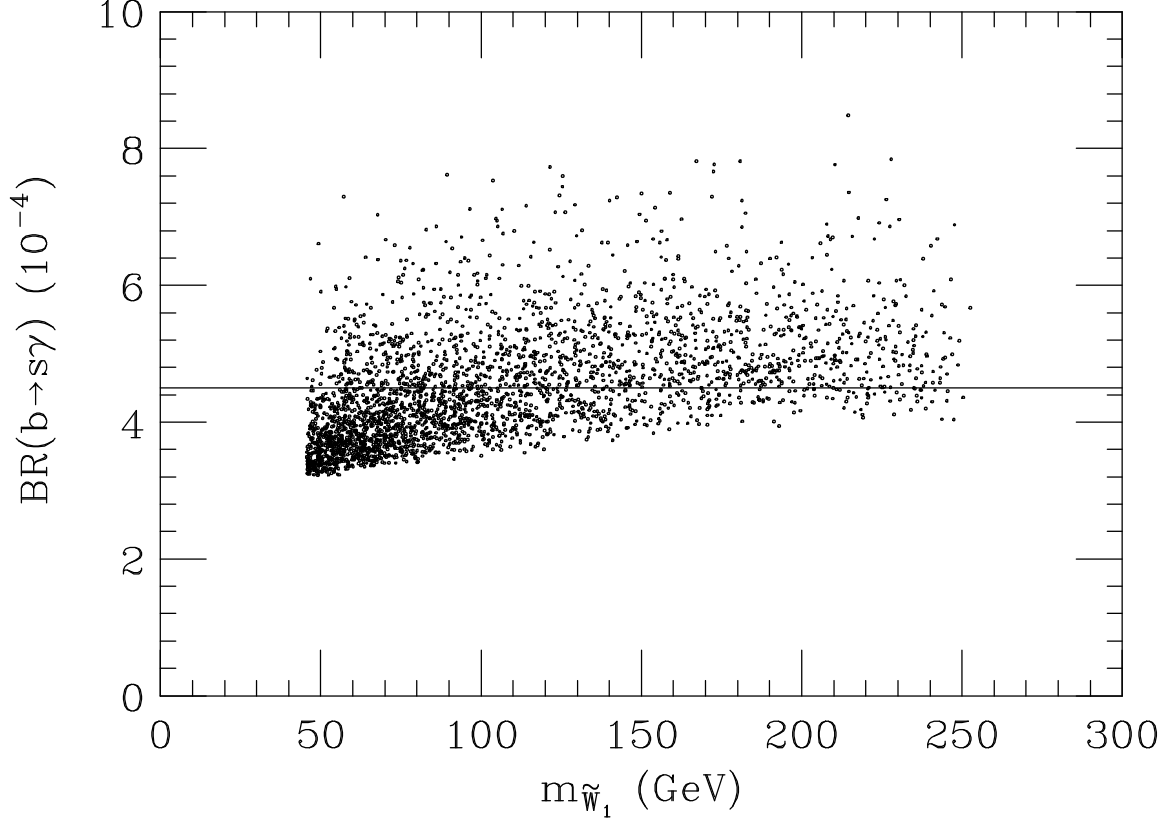


FIG. 10. Branching ratio $B(b \rightarrow s\gamma)$ as a function of the light chargino mass when the input parameters are varied within the intervals given in Eq. (2.1). These points in parameter space are characterized by small $|A_t|$, which favours small values of $B(b \rightarrow s\gamma)$ when $\tan\beta$ is large.

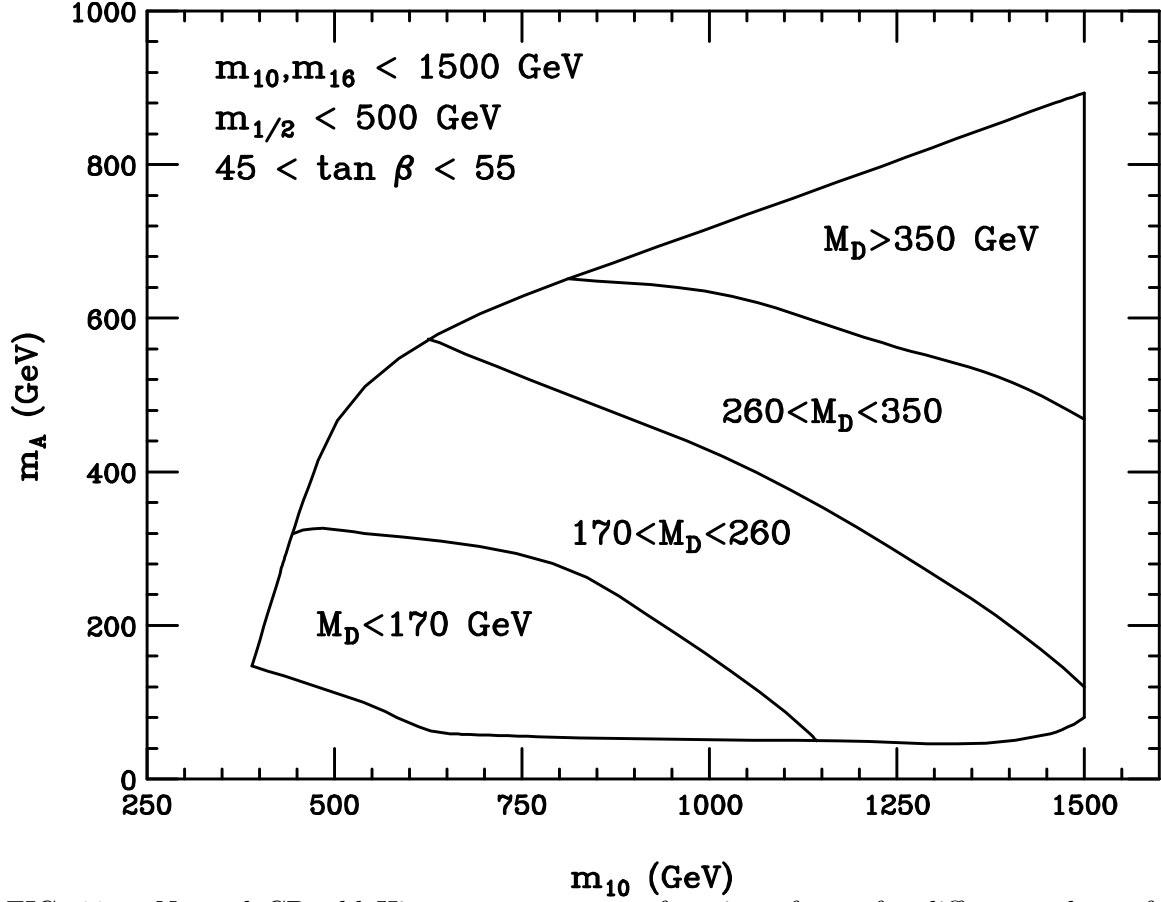


FIG. 11. Neutral CP-odd Higgs mass m_A as a function of m_{10} for different values of the D-term parameter M_D . The heavy neutral CP-even Higgs H has a mass very close to m_A except when $m_A < 100 \text{ GeV}$.

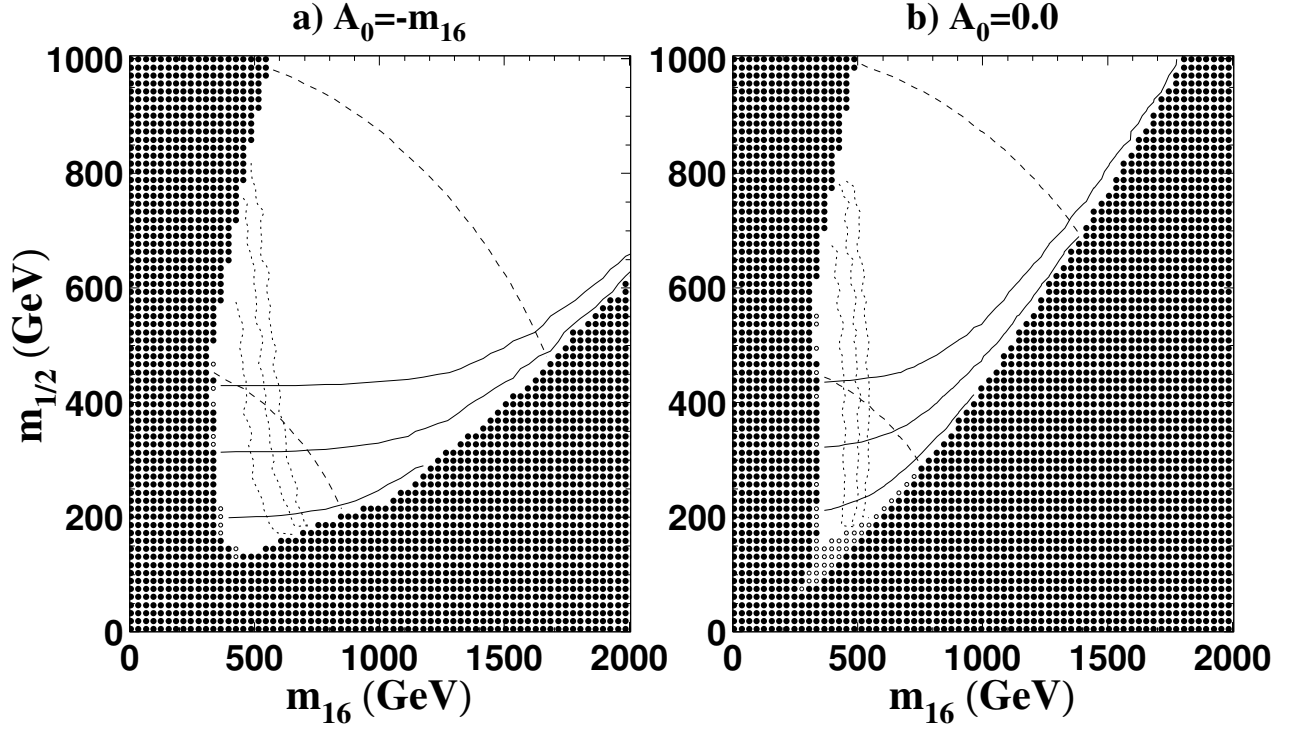


FIG. 12. The same parameter space planes as in Fig. 4, but now showing regions of parameter plane where 5σ $b\bar{b}A$ and $b\bar{b}H$ signals may be seen with the $D0$ detector at Fermilab Tevatron for (contours from left to right) integrated luminosities of 2, 10 and 30 fb^{-1} .

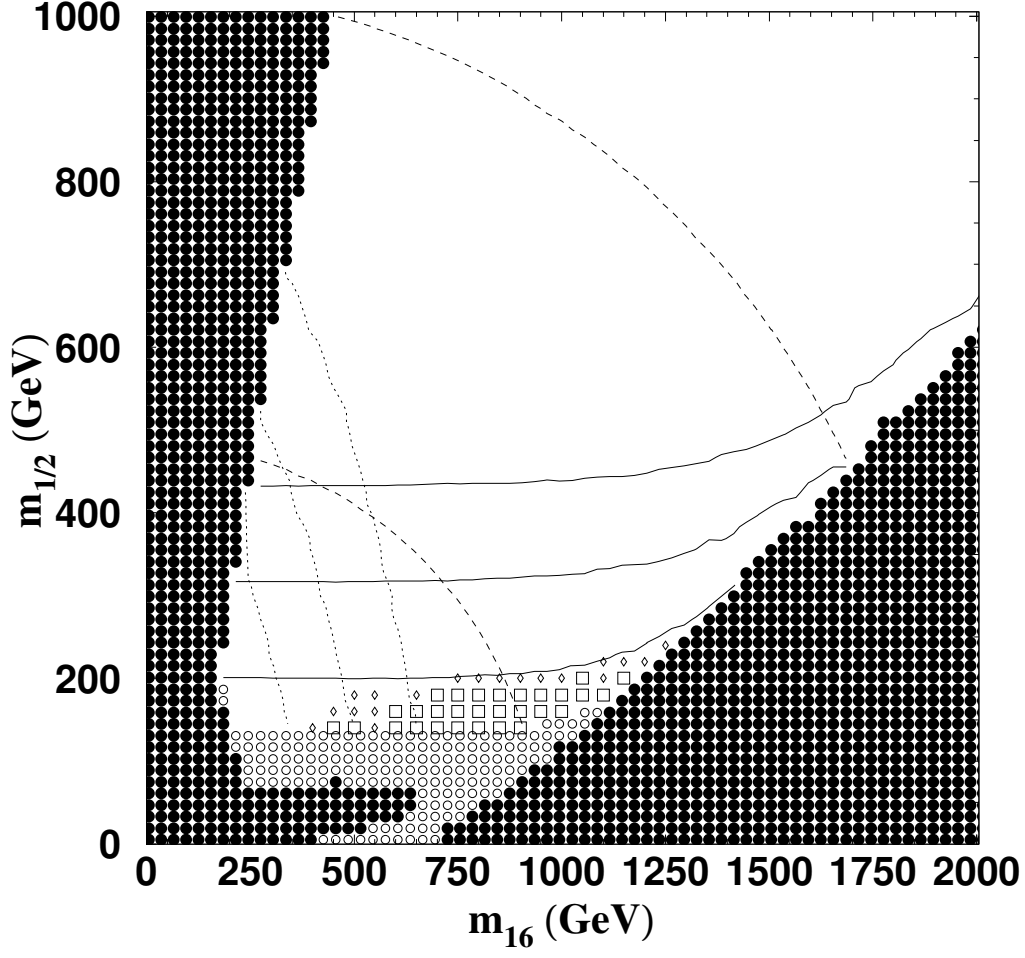


FIG. 13. Regions of the m_{16} *vs.* $m_{1/2}$ parameter plane where trilepton signals may be seen at the Fermilab Tevatron. Open squares can be seen at the 5σ level with 25 fb^{-1} of data, while diamonds can be seen at the 3σ level. We take $A_0 = 0$, $\tan\beta = 47$, $m_{10} = 1.14m_{16}$, $M_D = \frac{1}{3}m_{16}$ and $\mu < 0$.

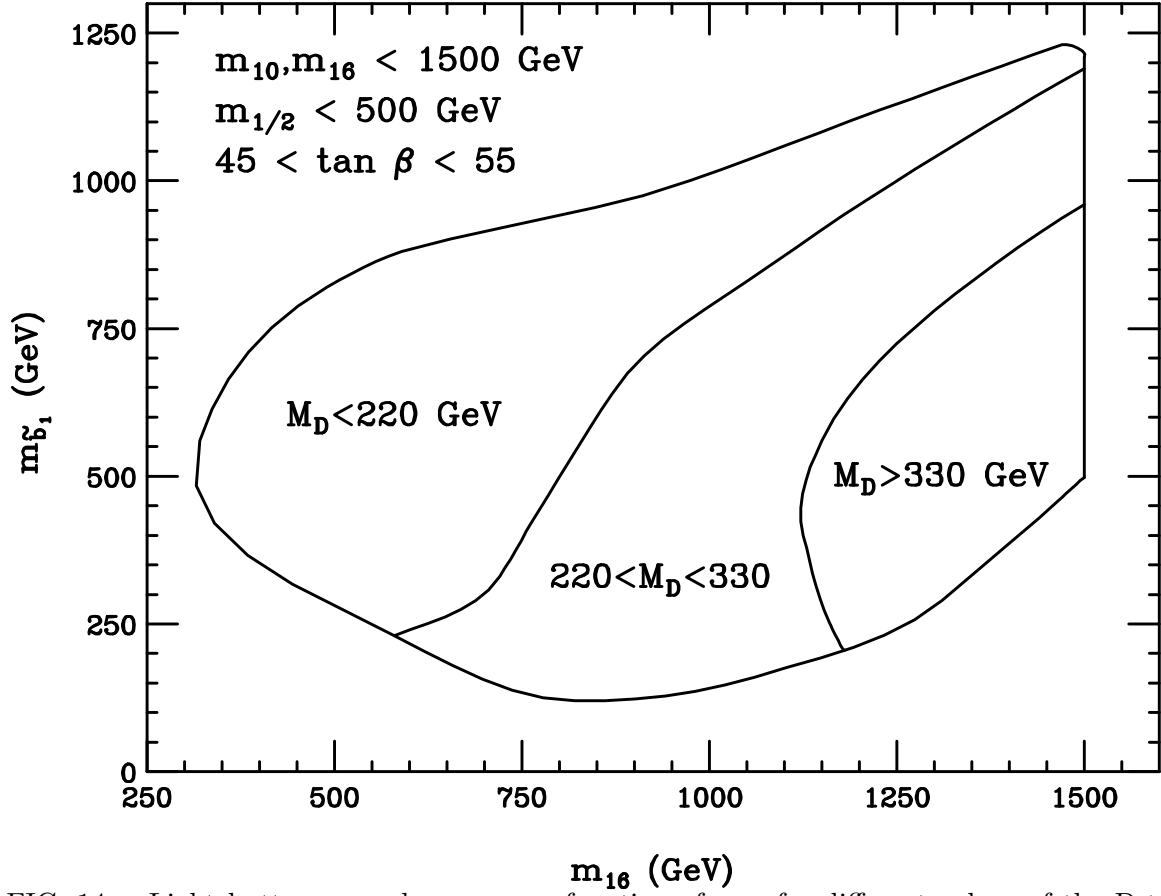


FIG. 14. Light bottom squark mass as a function of m_{16} for different values of the D-term parameter M_D . Very light sbottoms can be obtained for intermediate values of M_D .

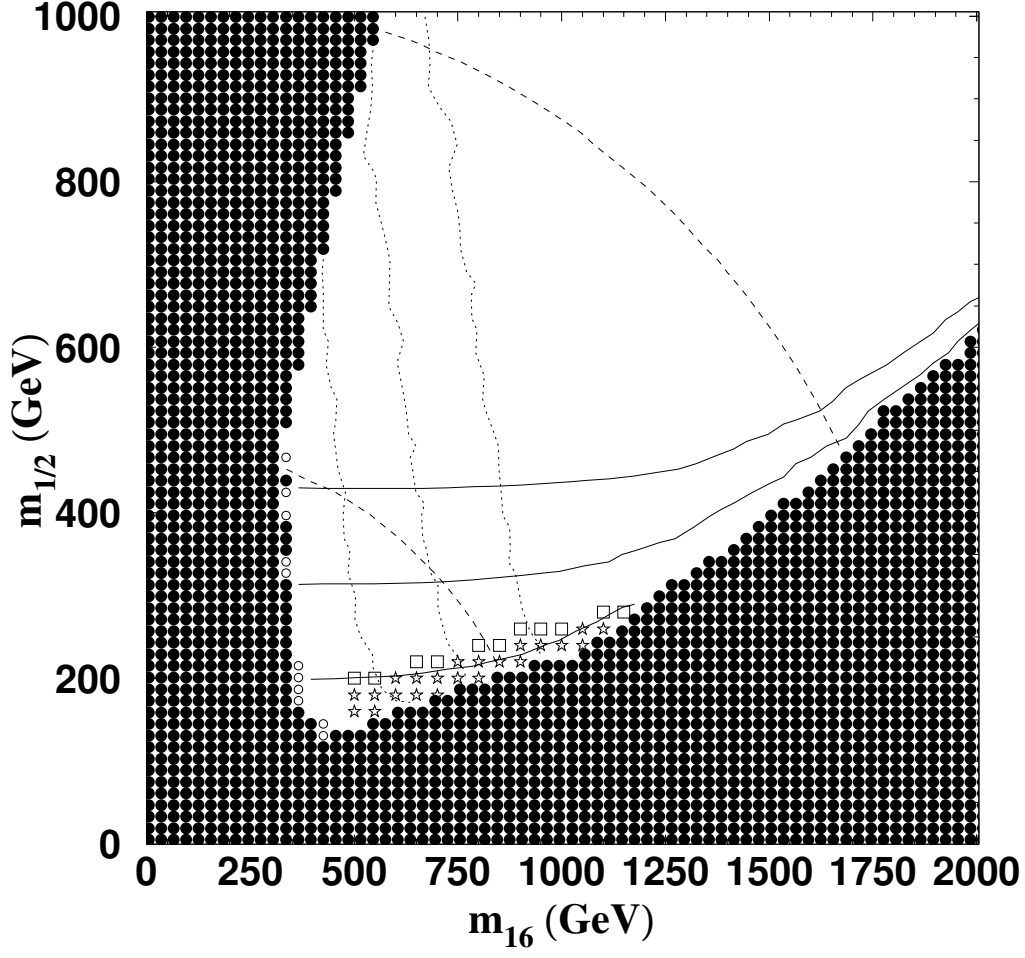


FIG. 15. Regions of the m_{16} vs. $m_{1/2}$ parameter plane where $\tilde{b}_1\tilde{b}_1 \rightarrow b\bar{b} + \cancel{E}_T$ events can be seen above background at the Fermilab Tevatron. The stars show points where a 5σ signal can be seen at Run 2 (2 fb^{-1}) and the open squares show points where a 5σ signal can be seen at Run 3 (25 fb^{-1}). We take $A_0 = -m_{16}$, $\tan\beta = 50$, $m_{10} = 1.25m_{16}$, $M_D = \frac{1}{3}m_{16}$ and $\mu < 0$.